APPLICATION OF THE LOGNORMAL DISTRIBUTION TO OPTICAL SPECTROSCOPY AND STUDIES OF ERRORS

By

CHE TED CHEN

A DISSERTATION PRESENTED TO THE GRADUATE COUNCIL
OF THE UNIVERSITY OF FLORIDA
IN PARTIAL FULFILLMENT OF THE REQUIREMENTS
FOR THE DEGREE OF DOCTOR OF PHILOSOPHY

UNIVERSITY OF FLORIDA

1976

ACKNOWLEDGEMENTS

The author wishes to acknowledge the financial supports from the Department of Chemistry, Dr. Rudi Avni and Dr. James D. Winefordner.

He is also grateful to Dr. James D. Winefordner for discussions on the spectral profiles and the signal-to-noise ratios, to Dr. Kuang-Pang Li for discussions on the gc peaks, to Dr. Shiro Matsumoto and Dr. David E. Metzler for providing the literature for the lognormal distribution, and to Dr. Mark C. Yang for discussions on statistics.

Gratitude should be given to his father for moral and financial support.

Without the encouragement and patience of his wife, this work would not have been possible.

TABLE OF CONTENTS

Abstract of Dissertation Presented to the
Graduate Council of the University of Florida
in Partial Fulfillment of the Requirements
for the Degree of Doctor of Philosophy

APPLICATION OF THE LOGNORMAL DISTRIBUTION TO OPTICAL SPECTROSCOPY AND STUDIES OF ERRORS

By

Che Ted Chen

December, 1976

Chairman: James D. Winefordner
Major Department: Chemistry

The lognormal distribution is a statistics for positive variables. It is applied to the positive physical quantities, such as transmitted irradiance, frequency, wavelength, etc.

It is shown that the transmitted irradiance to be determined is not identical to the quantity that is measured. The way to cover the error is discussed. The lognormal distribution explains the red-shift, asymmetry and broadening of a spectral profile. It also explains why the reaction rate constant is not a constant and interprets the bending of the analytical growth curve.

CHAPTER I
INTRODUCTION

The lognormal distribution, in its simplest form, may be defined as a variable whose logarithm obeys the normal law of probability.[1] The related literature is large, and appears under a variety of names - the Galton-McAlister, Kapteyn or Gibrat distribution, the logarithmico-normal or simply the lognormal distribution. The general properties of the lognormal distribution have been well studied and reviewed.[1-20] It has found applications in small particle statistics, e.g., distribution of particle sizes;[21-38] in economics, e.g., distribution of prices, sales volumes, incomes, etc.;[1,19,39-49] in biology and anthropology, e.g., weights of human beings;[4,6,12,15,50-64] in analysis of the abundances of species, e.g., trace concentrations in rocks;[65-77] in engineering, e.g., mechanical or electrical lifetimes of materials;[18,78-89] in philology, e.g., distributions of the radical components of Chinese characters;[1,90-94] and in physics, e.g., distributions of neutrons slowed by elastic impacts.[95,96] During the past decade, the applications of the lognormal distribution have included studies of irradiance distributions of electromagnetic waves passing through or scattered by inhomogeneous media, and analysis of the band shapes of molecular spectra.[97-129]

The lognormal distribution has different forms.[1] In its simplest form, the lognormal is better than the normal distribution for positive quantities.[16,18] The detailed theory of the lognormal distribution will not be given here. However, an example will be given to show why the normal distribution "is strictly applicable only if . . . . negative measurements are possible."[18] The example, given here, is a study of the wordlengths (numbers of letters per word) on page 1 from a book written by H. A. Laitinen.[130] There are 304 words and 1717 letters in that page. The average wordlength and the standard deviation of the wordlengths are 5.65 and 3.49 letters per word, respectively. The distribution of the wordlengths is shown in Figure 1-1. If it were assumed that the wordlength followed the normal distribution with the average wordlength being 5.65 and the standard deviation being 3.49, as shown in Figure 1-2, then one would expect from the normal distribution that there should be some words with negative wordlengths. However, negative wordlengths are impossible. It is clear in the above example that the normal distribution is inapplicable because negative measurements of wordlengths are impossible.

In the simplest lognormal distribution, according to the definition, the logarithm of a positive variable, rather than the variable itself, follows the normal distribution. For example, if the pH values of a solution follow the normal distribution, then the activities of the hydronium ions follow the lognormal distribution. One of the fundamental properties

The lognormal distribution has different forms.[1] In its simplest form, the lognormal is better than the normal distribution for positive quantities.[16,18] The detailed theory of the lognormal distribution will not be given here. However, an example will be given to show why the normal distribution "is strictly applicable only if . . . . negative measurements are possible."[18] The example, given here, is a study of the wordlengths (numbers of letters per word) on page 1 from a book written by H. A. Laitinen.[130] There are 304 words and 1717 letters in that page. The average wordlength and the standard deviation of the wordlengths are 5.65 and 3.49 letters per word, respectively. The distribution of the wordlengths is shown in Figure 1-1. If it were assumed that the wordlength followed the normal distribution with the average wordlength being 5.65 and the standard deviation being 3.49, as shown in Figure 1-2, then one would expect from the normal distribution that there should be some words with negative wordlengths. However, negative wordlengths are impossible. It is clear in the above example that the normal distribution is inapplicable because negative measurements of wordlengths are impossible.

In the simplest lognormal distribution, according to the definition, the logarithm of a positive variable, rather than the variable itself, follows the normal distribution. For example, if the pH values of a solution follow the normal distribution, then the activities of the hydronium ions follow the lognormal distribution. One of the fundamental properties

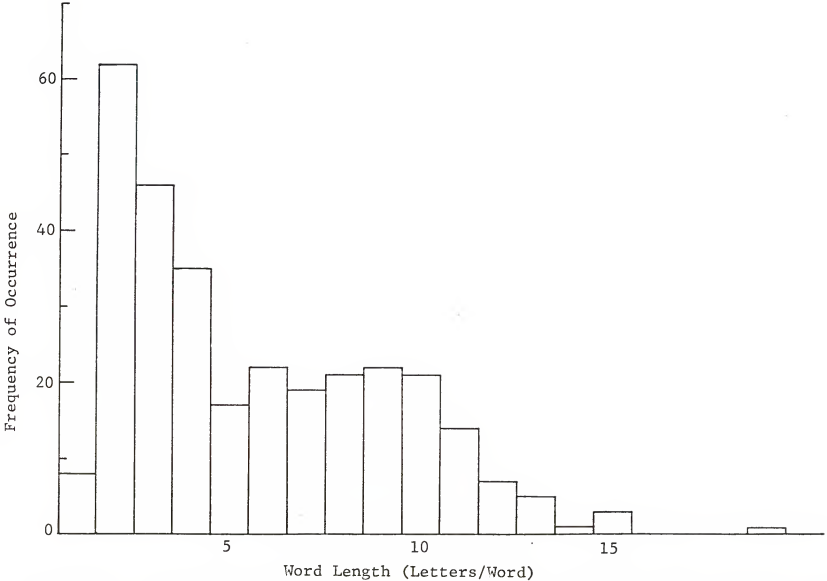

Fig. 1-1 - Actual Distribution of Word Length (Mean = 5.69; Standard Deviation = 3.49)

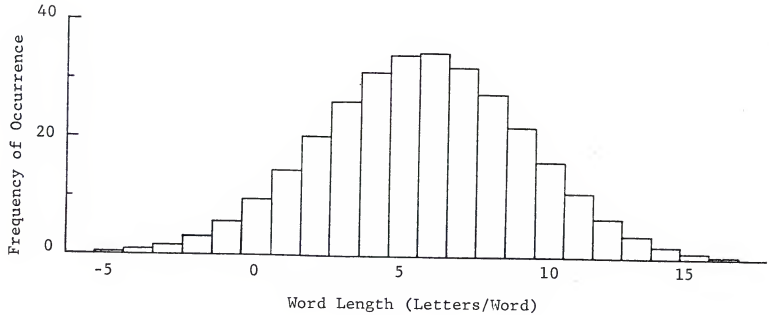

Fig. 1-2 - Normal Distribution of Word Length (Mean = 5.69; Standard Deviation = 3.49)

of the lognormal distribution is that the average of a variable does not represent the value of that variable when there is no disturbance of the variable.[1,18] In this case, for a positive variable, the random error will "not follow the normal law of error (the normal distribution), which is the fundamental starting point for analysis of data."[130] Even by taking the average of sufficient observations, it is impossible to overcome the scatter (with limits) so that the accuracy will not be affected. To help recognize this problem in the lognormal distribution, but not to justify it theoretically, an example of exaggeration will be given here. Suppose there is a solution with its pH value being 2. If the measured pH values, due to some unknown factors, are 1, 2, and 3, the average pH value can be reported as 2, and the average activity of the hydronium ions may be reported as 0.01. However, from the same pH values, 1, 2, and 3, the activities of the hydronium ions can be expressed as 0.1, 0.01, and 0.001, respectively. Therefore, the average activity of the hydronium ions may also be reported as $(0.1 + 0.01 + 0.001)/3 = 0.037$, which is quite different from 0.01 (pH = 2). The same problem might happen in absorption spectroscopy, due to the linear relationship between the concentration of the absorbing sample and the logarithm of the transmitted intensity (or photon flux). If the sample concentration in the optical region of the sample cell approximately follows the normal distribution, then the transmitted intensity would follow the lognormal distribution.[97-122]

The objective of Part I of this thesis is to apply the lognormal distribution to analytical optical spectroscopy and to the study of indeterminate errors in analytical optical spectroscopy. Part II covers the determinate errors caused by the multiple reflections within the cell.

PART I

APPLICATIONS OF THE LOGNORMAL DISTRIBUTION TO OPTICAL SPECTROSCOPY AND STUDIES OF INDETERMINATE ERRORS

CHAPTER II
LOGNORMAL DISTRIBUTION OF THE IRRADIANCES OF AN OPTICAL WAVE AFTER PASSING THROUGH A RANDOM MEDIUM

The problem will be first treated with a binomial model and then with a random walk model. Eventually, the lognormal distribution of the transmitted irradiances (intensities or photon fluxes) of an optical wave passing through a turbulent medium is derived without the use of the complicated theory of electromagnetic waves, assuming the numbers of the filters (absorbers or optical attenuators) in the optical region follow the normal distribution.[97-122] Expressions for inaccuracies, signals and noises are derived.

Binomial Model

In order to understand the basic properties of the lognormal distribution, it is helpful to picture an optical medium as composed of four adjoining cells for the illustration. Under the condition of no turbulence, each of the four cells is assumed to contain a filter (or absorber), with the same transmittance, t. The light source, S, assumed to be monochromatic, gives off a parallel beam of radiation with an incident irradiance I_{oo} (s^{-1}). After passing through the homogeneous medium with one filter in each of the four cells

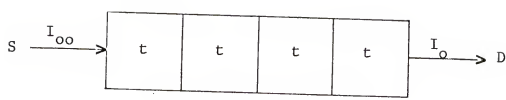

Fig. 2-1 - Hypothetical Homogeneous Medium
S: Light Source; D: Detector;
I_{oo}: Incident Irradiance; I_o Transmitted
Irradiane; t: Transmittance of the Filter

as shown in Figure 2-1, the irradiance of the transmitted light, I_o (s^{-1}), is given by

$$I_o = t^4 I_{oo} \tag{2-1}$$

The absorbance of the homogeneous medium, A_o, is given by

$$A_o = \log \left(\frac{I_{oo}}{I_o}\right) = -4 \log t \tag{2-2}$$

However, under the condition of turbulence, each cell is assumed to be statistically identical and independent, and to have equal probability of either gaining an extra filter or losing one. The combinations of the possible occurrence of gaining or losing a filter in each of the four cells are shown in Table 2-1, where"+"denotes that the cell gains one more filter or contains two filters, and"-"denotes that the cell loses one filter or contains no filter. In Table 2-2, the relative frequencies of occurrences and the expressions for the transmitted irradiances in the turbulent medium are given. The relative frequency versus the overall transmittance of the turbulent medium in Table 2-2 is plotted in Figure 2-2 for t = 0.7 and I_{oo} = 1, as an example. The average transmitted irradiance, I_{ave}, of the turbulent medium, is given by

$$I_{ave} = \frac{1}{16} (t^8 + 4\, t^6 + 6\, t^4 + 4\, t^2 + 1)$$

$$= \frac{(1 + t^2)^4}{16} I_{oo} \tag{2-3}$$

So the absorbance of the inhomogeneous medium, A_{in}, is given by

Table 2-1

Possible Combinations and Number of Filters in the Turbulent Medium

Possible Combination				Number of Filters in the Medium
+	+	+	+	8
+	+	+	-	6
+	+	-	+	6
+	+	-	-	4
+	-	+	+	6
+	-	+	-	4
+	-	-	+	4
+	-	-	-	2
-	+	+	+	6
-	+	+	-	4
-	+	-	+	4
-	+	-	-	2
-	-	+	+	4
-	-	+	-	2
-	-	-	+	2
-	-	-	-	0

Table 2-2

The Relative Frequency of
Occurrence and the Transmittance

Relative Frequency	Transmittance (I/I_{oo})	Absorbance $\log (I_{oo}/I)$
1	t^8	$-8 \log t$
4	t^6	$-6 \log t$
6	t^4	$-4 \log t$
4	t^2	$-2 \log t$
1	1	0

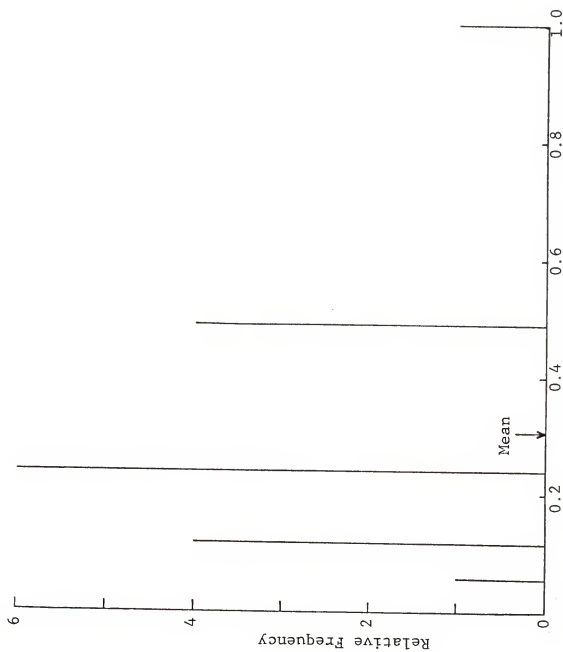

Fig. 2-2 - Relative Frequency and Transmittance of a Turbulent Medium ($t = 0.7$)

$$A_{in} = \log \left(\frac{I_{oo}}{I_{ave}}\right) = -4 \log \left(\frac{1 + t^2}{2}\right) \qquad (2\text{-}4)$$

For t = 0.7, we have, from Equations (2-1), (2-2), (2-3), and (2-4),

$$I_{ave} = 0.31\ I_{oo}$$

$$A_{in} = 0.51$$

$$I_o = 0.24\ I_{oo}$$

$$A_o = 0.62$$

It is clear that the average transmitted irradiance, I_{ave} (s^{-1}), of an inhomogeneous medium, is greater than the transmitted irradiance of a homogeneous medium, I_o, and the absorbance of an inhomogeneous medium, A_{in}, is smaller than the absorbance of a homogeneous medium, A_o. Therefore, in the spectroscopic determination of the concentration such as in a turbulent flame or in a stop-flow technique, the turbulence will result in a lower value. The relative error of the absorbance, E_A, is

$$E_A = \frac{A_{in} - A_o}{A_o} = \frac{\log (1 + t^2) - \log (2t)}{\log t} \qquad (2\text{-}5)$$

The geometrical mean of the transmitted irradiance, I_g, is

$$I_g = [t^8 \times (t^6)^4 \times (t^4)^6 \times (t^2)^4 \times 1]^{1/16}\ I_{oo}$$

$$= t^4\ I_{oo} = I_o \qquad (2\text{-}6)$$

Thus the geometrical mean of the transmitted irradiances in turbulent medium is equal to the transmitted irradiance in the homogeneous medium. The relative frequency versus log (I/I_{oo})

is plotted in Figure 2-3. It can be seen that in Figure 2-3 the distribution is symmetric about the mean, while the distribution in Figure 2-2 is not symmetric. From the mean in Figure 2-3, the absorbance, A_{ave}, is given by

$$A_{ave} = -\frac{1}{16}[\log (t^8) + 4 \log (t^6) + 6 \log (t^4) + 4 \log (t^2)]$$

$$= -4 \log t = A_o \qquad (2\text{-}7)$$

Thus the average absorbance is equal to the absorbance of the homogeneous medium. Equation (2-6) or (2-7) should be used to avoid errors due to the turbulence of the medium. In practice, Equation (2-6) is inconvenient. It is advisable, from Equation (2-7), to take the average after the signals are converted to absorbances. The standard deviation of the transmitted irradiances, σ_I, is

$$\sigma_I = \left[\frac{(1 + t^4)^4}{16} - \frac{(1 + t^2)^8}{256}\right]^{\frac{1}{2}} I_{oo} \qquad (2\text{-}8)$$

Similarly, if the turbulent medium consists of n cells, the average transmitted irradiance, I_{ave}, and the standard deviation of the transmitted irradiances, σ_I, are given by, respectively

$$I_{ave} = \frac{(1 + t^2)^n}{2^n} I_{oo} \qquad (2\text{-}9)$$

and

$$\sigma_I = \left[\frac{(1 + t^4)^n}{2^n} - \frac{(1 + t^2)^{2n}}{2^{2n}}\right]^{\frac{1}{2}} I_{oo} \qquad (2\text{-}10)$$

The absorbance of the homogeneous medium, A_o, is

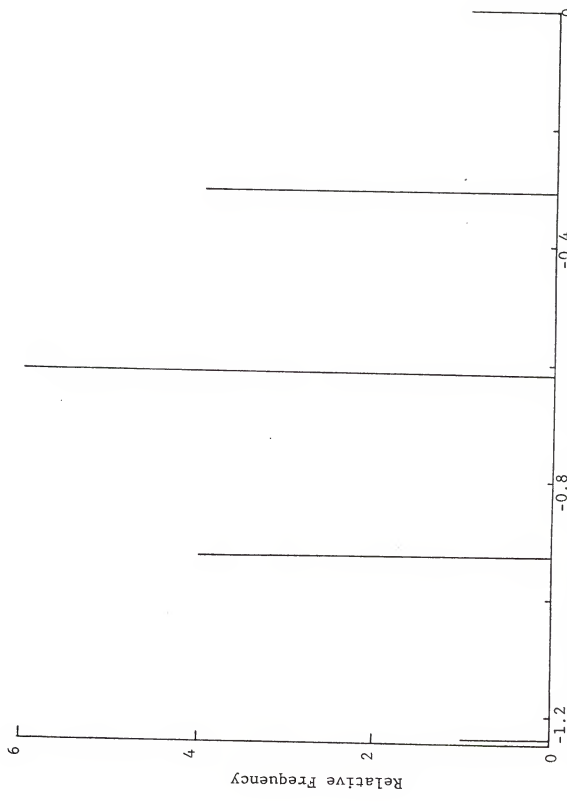

Fig. 2-3 - Distribution of the Transmitted Irradiances on the Logarithmic Scale

$$A_o = -n \log t \tag{2-11}$$

The absorbance of the inhomogeneous medium, A_{in}, is

$$A_{in} = \log \frac{I_{oo}}{I_{ave}} = n \log \left(\frac{2}{1 + t^2}\right) \tag{2-12}$$

A_o and A_{in} versus n for t = 0.7 are plotted in Figure 2-4. The relative error of the absorbance, E_A, is given by

$$E_A = \frac{A_{in} - A_o}{A_o} = \frac{\log (1 + t^2) - \log (2t)}{\log t} \tag{2-13}$$

It can be seen that the relative error of the absorbance is independent of the numbers of the cells in the medium, n, and that it decreases as the transmittance of each filter, t, becomes larger as shown in Figure 2-5. If the optical activity coefficient of the filter in the turbulent medium, a, can be defined as

$$a = \frac{A_{in}}{A_o}$$

then

$$a = \frac{\log (1 + t^2) - \log 2}{\log t} \tag{2-14}$$

It is clear that the activity coefficient is dependent on the transmittance of each filter. The ratio of the average transmitted irradiance of the inhomogeneous medium, I_{ave}, to that of the homogeneous medium, I_o, is given by

$$\frac{I_{ave}}{I_o} = \frac{(1 + t^2)^n}{2^n t^n} \tag{2-15}$$

I_{ave}/I_o versus the transmittance of each filter, t for various

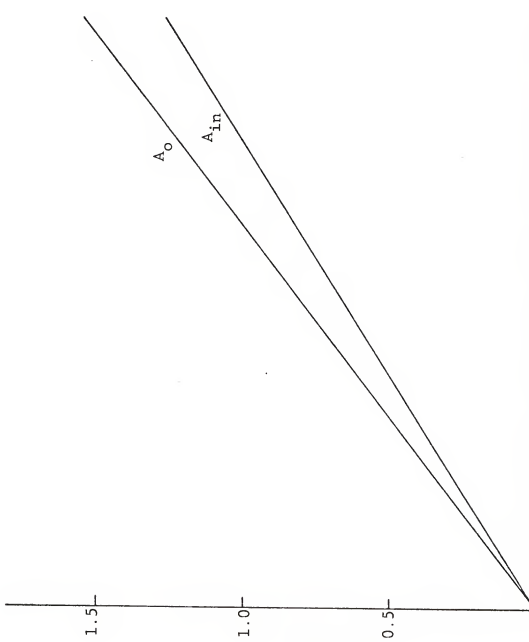

Fig. 2-4 - Absorbances of a Homogeneous and an Inhomogeneous Medium ($\tau = 0.7$)

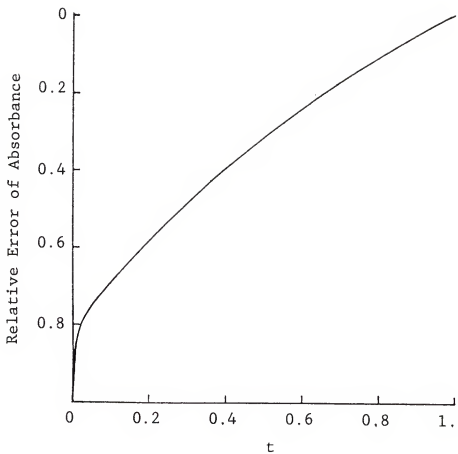

Fig. 2-5 - Relative Error of Absorbance

media is plotted in Figure 2-6. It can be seen that the irradiance ratio increases as the numbers of cells become larger, or as the transmittance of each cell becomes smaller. The signal-to-noise ratio of irradiance, S/N, is given by

$$\frac{S}{N} = \frac{I_{ave}}{\sigma_I} = \frac{(1 + t^2)^n}{[(1 + t^4)^n 2^n - (1 + t^2)^{2n}]^{\frac{1}{2}}} \qquad (2\text{-}16)$$

S/N versus n, for various t are plotted in Figure 2-7, from which we can see that the signal-to-noise ratio decreases as n increases or t becomes smaller. For n = 10, t = 0.9, the relative frequencies of occurrence versus I/I_{oo} and log (I/I_{oo}) are plotted in Figures 2-8 and 2-9, respectively. The distribution of I, in Figure 2-8. is skewed to the right, in other words, positively skewed, or the dominant tail of the distribution is on the right while the distribution of log (I/I_{oo}) as shown in Figure 2-9, is symmetric about the mean.

Substituting t = 0.7 into Equation (2-13) gives

$$E_A = \frac{A_{in} - A_o}{A_o} = -0.18$$

The above equation indicates that in absorption spectroscopy, the absorbance would have a lower value due to the turbulence of the optical medium. Substituting n = 4 and t = 0.7 into Equation (2-15) gives

$$I_{ave} = 1.33\ I_o$$

The above equation indicates that in fluorescence spectroscopy, the fluorescence signal would have a lower value because more

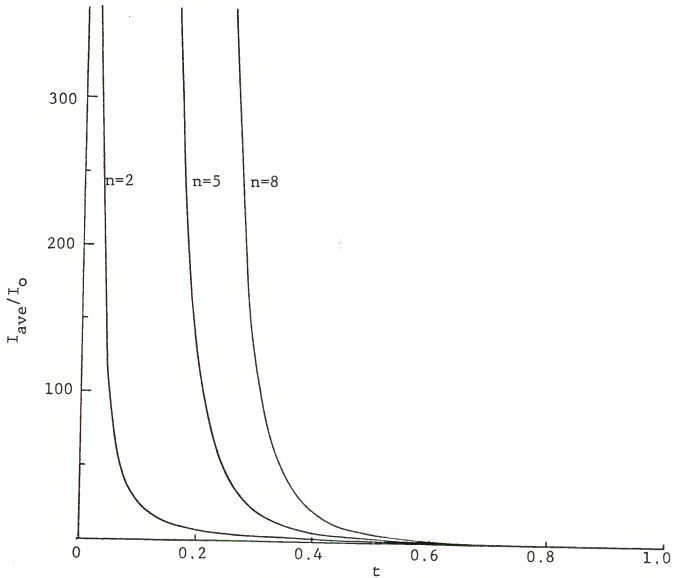

Fig. 2-6 - Dependence of Irradiance Ratio on the Number of Cells and the Transmittance of the Filter

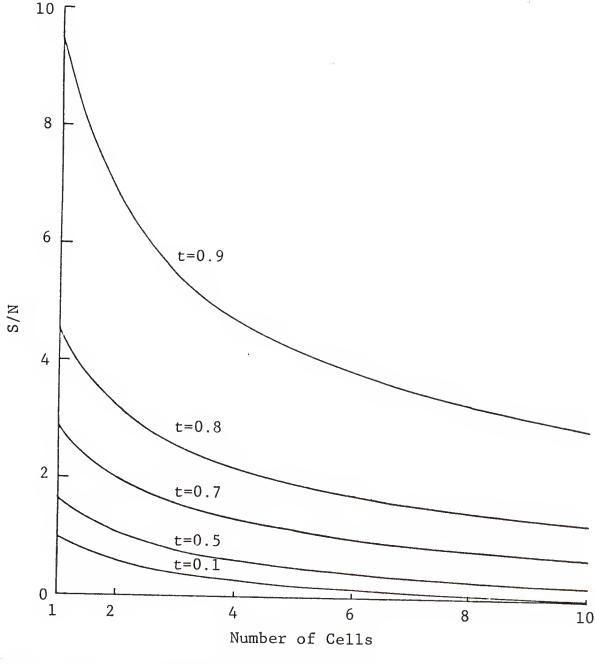

Fig. 2-7 - Dependence of the Signal-To-Noise Ratio on the Number of Cells and the Transmittance of the Filter

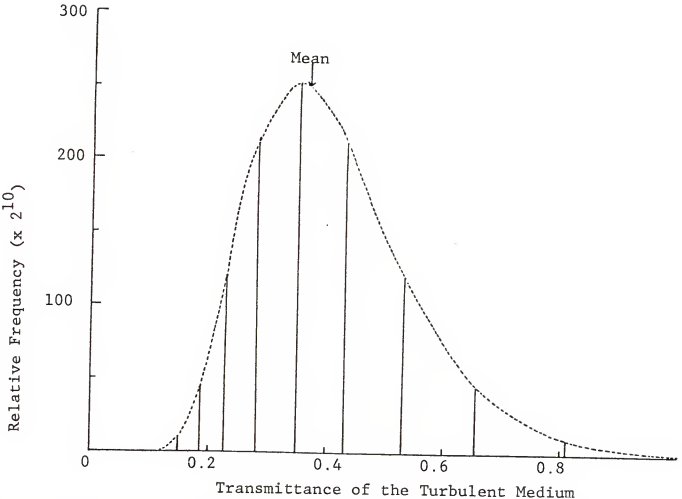

Fig. 2-8 - Distribution of the Transmittance of the Turbulent Medium (n = 10; t = 0.9; Dotted Curve is the Envelope of the Distribution)

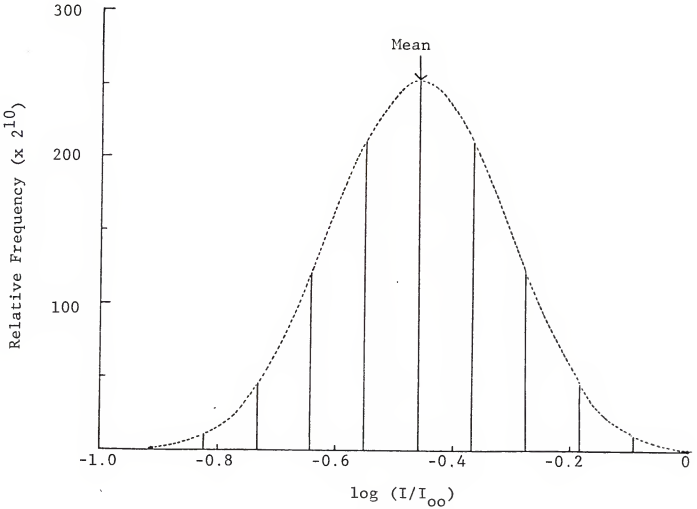

Fig. 2-9 - Distribution of the Logarithm of the Transmitted Irradiance in the Turbulent Medium (n = 10; t = 0.9; Dotted Curve is the Envelope of the Distribution)

light would pass through a turbulent medium than a homogeneous medium.

Now, let us consider the inhomogeneous medium as consisting of (n + h) cells of which n cells suffer turbulence, while h cells suffer no turbulence, then

$$I_{ave} = \frac{(1 + t^2)^n}{2^n} t^h I_{oo} \tag{2-17}$$

$$\sigma_I = [\frac{(1 + t^4)^n}{2^n} - \frac{(1 + t^2)^{2n}}{2^{2n}}]^{\frac{1}{2}} t^h I_{oo} \tag{2-18}$$

$$I_o = t^{n + h} I_{oo} \tag{2-19}$$

$$\frac{I_{ave}}{I_o} = \frac{(1 + t^2)^n}{2^n t^n} \tag{2-20}$$

$$I_g = I_o \tag{2-21}$$

$$\frac{S}{N} = \frac{(1 + t^2)^n}{[(1 + t^4)^n 2^n - (1 + t^2)^{2n}]^{\frac{1}{2}}} \tag{2-22}$$

$$A_o = -(n + h) \log t \tag{2-23}$$

$$A_{in} = -h \log t - n \log (\frac{1 + t^2}{2}) \tag{2-24}$$

and

$$E_A = \frac{A_{in} - A_o}{A_o} = \frac{\log (1 + t^2) - \log (2t)}{(n + h) \log t} \tag{2-25}$$

It is interesting to note that Equations (2-15) and (2-20) are identical, and that Equations (2-16) and (2-22) are identical, even though they apply to different conditions. We can see that I_{ave}/I_o and S/N are independent of the numbers of cells, h, which suffer no turbulence. The geometrical mean of the

transmitted irradiances, I_g, is equal to I_o. The relative error of absorbance, E_A, decreases as t increases.

However, the binomial model has the mathematical inconvenience in computations. Because the experimental evidences indicate a lognormal distribution of irradiances, an approximate approach to the lognormal distribution will be given in the following section based on the random walk model.

Random Walk Model

We will assume the medium as composed of k cells, of which n cells suffer turbulence and the rest (k - n) of the cells suffer no turbulence. To start the discussion, consider that no cells suffer turbulence, so the transmitted irradiance, I_o, is given by

$$I_o = t^k I_{oo} \tag{2-26}$$

If only one cell suffers turbulence, the transmitted irradiance, I_1, is given by

$$I_1 = t^{k \pm 1} I_{oo}$$

$$= t^{\pm a_1} I_o$$

where $a_1 = \pm 1$.

If j cells of the total k cells suffer turbulence, then

$$I_j = t^{k \pm 1 \pm 1 \ldots . \pm 1 \pm 1} I_{oo}$$

$$I_j = t^{-\sum_1^j a_j} I_o$$

where $a_j = \pm 1$.

In our model, n cells of the total k cells are assumed to suffer turbulence, so the irradiance, I, reaching the surface of the detector is given by

$$I = t^{-\sum_1^n a_j} I_o \tag{2-27}$$

or

$$\sum_1^n a_j = \frac{1}{\ln t} \ln \frac{I_o}{I} \tag{2-28}$$

For simplicity, define

$$N = \sum_1^n a_j \tag{2-29}$$

where N is the summation of n random numbers of ± 1, then

$$N = \frac{1}{\ln t} \ln \frac{I_o}{I} \tag{2-30}$$

The combinations of n random numbers of ± 1 will be treated with the random walk model as shown in Figure 2-10, using the Galton board for illustration.[131] In this apparatus, small balls of equal diameter run down a slightly inclined plane, passing through n horizontal rows of pins arranged in such a way that a network of equilateral triangles is formed. All balls are released at the same spot, x = 0, above the central pin of the first row. The diameter of the balls is slightly smaller than the distance between two neighboring pins, the latter distance may be taken as two units. It is assumed that each ball when hitting a nail (of any row) will deviate by

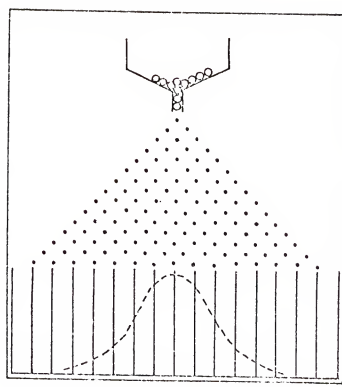

Fig. 2-10 - The Galton Board

one unit to the right or to the left with equal probabilities, 1/2. Each ball, after passing through the n rows of pins, will come to rest in one of the compartments (the width of each being equal to two units) at the bottom of the board. The probability, $P_2(N)$, that a ball arrives in the compartment the acscissa of whose midpoint, N, which is the summation of n random numbers of ±1, is given by [131,132]

$$P_2(N) = \frac{n!}{[\frac{1}{2}(n+N)]![\frac{1}{2}(n-N)]!}\left(\frac{1}{2}\right)^n \qquad (2\text{-}31)$$

where N, the summation of n random numbers of ±1, is a positive or negative number equal to the following[131,132]

$$-n, -n+2, -n+4, \ldots\ldots, n-4, n-2, n$$

When N is sufficiently large, Equation (2-31) becomes approximately[131,132]

$$P_2(N) = \frac{\sqrt{2}}{\sqrt{\pi n}} \exp\left(-\frac{N^2}{2n}\right) \qquad (2\text{-}32)$$

A numerical comparison of the two Equations (2-31) and (2-32) is duplicated in Table 2-3 for n = 10.[131] The probabilities, calculated from Equation (2-31), are shown by the histogram in Figure 2-11. When the width of each compartment is unity, we have the probability[132]

$$P(N) = \frac{P_2(N)}{\int_{-\infty}^{\infty} P_2(N)\, dN}$$

$$= \frac{1}{\sqrt{2\pi n}} \exp\left(-\frac{N^2}{2n}\right) \qquad (2\text{-}33)$$

From Equations (2-30) and (2-31), we have the probability

Table 2-3

The Problem of Random Walk for n = 10

Position N	Probability from Eq. (2-31)	Probability from Eq. (2-32)
0	0.24609	0.252
2	0.20508	0.207
4	0.11715	0.113
6	0.04374	0.042
8	0.00977	0.010
10	0.00098	0.002

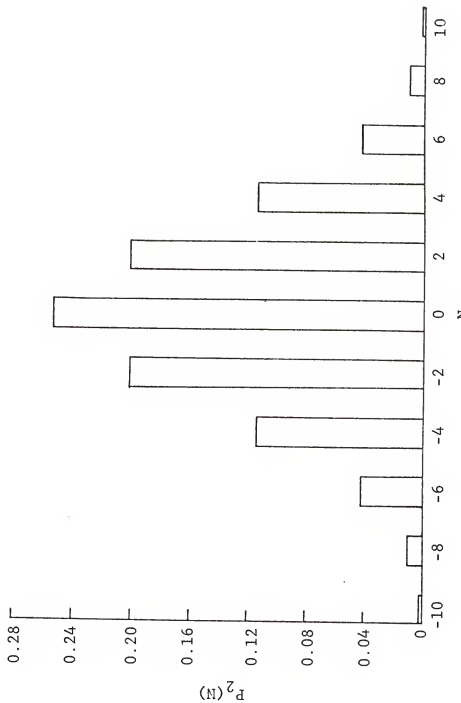

Fig. 2-11 - The Probability in Random Walk

density function of the transmitted irradiances[133,134]

$$P(I) = P(N) \left|\frac{dN}{dI}\right|$$

$$= -\frac{1}{\sqrt{2\pi n}\ \ln t\ I} \exp\left[-\frac{1}{2n \ln^2 t} \ln^2 \left(\frac{I}{I_o}\right)\right] \qquad (2\text{-}34)$$

Empirically, the lognormal density function takes the form

$$P(I) = \frac{1}{\sqrt{2\pi}\ \beta\ I} \exp\ -\frac{1}{2\beta^2} \ln^2 \left(\frac{I}{I_o}\right) \qquad (2\text{-}35)$$

where β is the characteristic parameter of the inhomogeneous medium.[123] Let $\beta = -\sqrt{n} \ln t$, and Equation (2-35) can be derived from Equation (2-34).

Equation (2-35) is plotted in Figure 2-12 for various values of β, and in Figure 2-13 for various values of I_o. The distributions of irradiances in both figures are skewed to the right. However, the probability density function of the distributions of the logarithms of irradiances, given by

$$P(\ln I) = P(I) \left|\frac{dI}{d \ln I}\right|$$

$$= \frac{1}{\sqrt{2\pi}\ \beta} \exp\left[-\frac{1}{2\beta^2} \ln^2 \left(\frac{I}{I_o}\right)\right] \qquad (2\text{-}36)$$

is symmetric about the mean and equal to $\ln I_o$. From Equation (2-35), the rth moment of I is given by[18]

$$U_r(I) = \int_0^\infty I^r\ P(I)\ dI$$

$$= I_o^r \exp\left(\frac{k^2 \beta^2}{2}\right) \qquad (2\text{-}37)$$

Hence, the arithmetic mean or the expected value of I, I_{ave},

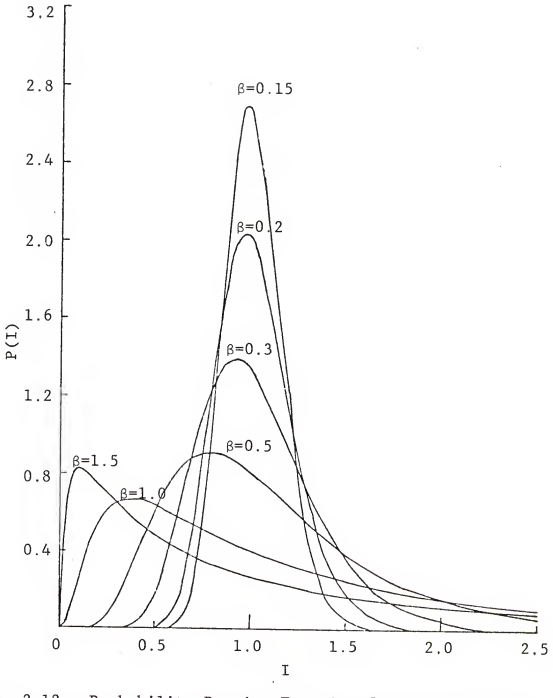

Fig. 2-12 - Probability Density Function for Various Values of I (I_o = 1)

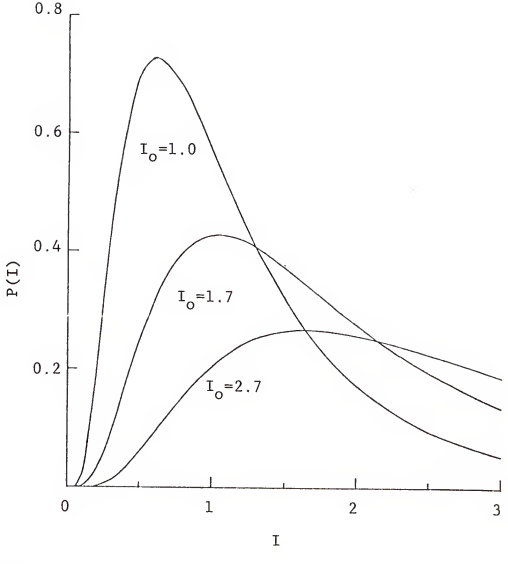

Fig. 2-13 - Probability Density Function for Various Values of I_o (β = 0.7)

is

$$I_{ave} = I_o \exp\left(\frac{\beta^2}{2}\right) \tag{2-38}$$

The above equation indicates that the average (measured) transmitted irradiance of an inhomogeneous medium, I_{ave}, is greater than the transmitted irradiance of a homogeneous medium, I_o. To overcome the error, due to the inhomogeneity of the medium, β should be measured and this requires additional work. From Equation (2-36), the average value of the logarithms of the transmitted irradiances of an inhomogeneous medium, $(\ln I)_{ave}$, is given by

$$(\ln I)_{ave} = \int_{I=0}^{I=\infty} \ln I \; P(\ln I) \; d(\ln I) = \ln I_o$$

Rearranging the equation above gives

$$I_o = \exp\left[(\ln I)_{ave}\right]$$

The above equation shows the error can be avoided if one takes the average value of the logarithms of the transmitted irradiances of an inhomogeneous medium.

The standard deviation of intensities, σ_I, is given by[18]

$$\begin{aligned}\sigma_I &= \int_0^\infty (I - I_{ave})^2 \, P(I) \, dI \\ &= I_o \exp\left(\frac{\beta^2}{2}\right) \left[\exp(\beta^2) - 1\right]^{\frac{1}{2}} \\ &= I_{ave} \left[\exp(\beta^2) - 1\right]^{\frac{1}{2}}\end{aligned} \tag{2-39}$$

It is interesting to note that the standard deviation of the intensity is proportional to the average intensity.

The first shape factor, γ_1, or skewness, given by

$$\gamma_1 = \frac{1}{\sigma_I^3} \int_0^\infty (I - I_{ave})^3 P(I)\, dI$$

$$= \gamma^3 + 3\gamma > 0 \qquad (2\text{-}40)$$

where $\gamma = [\exp(\beta^2) - 1]^{\frac{1}{2}}$ is for the simplicity of the expression, indicates that all the lognormal distribution is skewed to the right as shown in Figures 2-12 and 2-13.[18] The second shape factor, γ_2, or kurtosis (peakedness), given by

$$\gamma_2 = \frac{1}{\sigma_I^4} \int_0^\infty (I - I_{ave})^4 P(I)\, dI$$

$$= 6\gamma^6 + 15\gamma^4 + 16\gamma^2 + 3 > 3 \qquad (2\text{-}41)$$

shows the lognormal density function is more peaked than the normal density function.[5,18] From Equations (2-40) and (2-41), it is seen that for small values of β, the shape factors of the lognormal function are close to their normal values, 0 and 3, respectively.[18] The approximate normal distribution, $P_N(I)$, obtained from the lognormal distribution, when β is small, is given by

$$P_N(I) = \frac{1}{\sqrt{2\pi}\,\beta\, I_o} \exp\left[-\frac{(I - I_o)^2}{2\beta^2 I_o^2}\right] \qquad (2\text{-}42)$$

It will be shown that Equation (2-42) is an approximation of Equation (2-35), when β is small. Let the difference between Equations (2-35) and (2-42) be

$$D(I) = \frac{1}{\sqrt{2\pi}\ \beta\ I} \exp\left[-\frac{1}{2\beta^2} \ln^2 \left(\frac{I}{I_o}\right)\right]$$

$$-\frac{1}{\sqrt{2\pi}\ \beta\ I_o} \exp\left[-\frac{1}{2\beta^2\ I_o^2} (I - I_o)^2\right] \qquad (2\text{-}43)$$

(i) When $I = I_o$,

$$D(I) = 0$$

(ii) When I is in the vicinity of I_o,

$$I \doteq I_o \qquad (2\text{-}44)$$

so

$$\ln^2\left(\frac{I}{I_o}\right) = \ln^2 \left(1 + \frac{I - I_o}{I_o}\right) \doteq \frac{(I - I_o)^2}{I_o^2}$$

(2-45)

Combining Equations (2-43), (2-44) and (2-45), gives

$$D(I) \doteq 0$$

(iii) When I is far from I_o, both the exponential terms in Equation (2-43) fall to zero, and so

$$D(I) \doteq 0$$

From Equation (2-35), the most probable irradiance, I_{max}, obtained from

$$\frac{dP(I)}{dI} = 0 \qquad (2\text{-}46)$$

is given by

$$I_{max} = I_o \exp(-\beta^2) \qquad (2\text{-}47)$$

From Equations (2-38) and (2-47), it can be seen that the average irradiance shifts towards right and the most probable irradiance shifts towards left as β increases. The maximum

of the lognormal density function, P_{max}, defined as

$$P_{max} = P(I_{max})$$

is given by

$$P_{max} = \frac{1}{\sqrt{2\pi}\ \beta\ I_o} \exp\ (\beta^2) \tag{2-48}$$

The above equation is plotted in Figure 2-14. It can be seen that P_{max} decreases and then increases as β increases. The signal-to-noise ratio, S/N, is given by

$$\frac{S}{N} = \frac{I_{ave}}{\sigma_I} = [\exp\ (\beta^2) - 1]^{-\frac{1}{2}} \tag{2-49}$$

Dependence of Signal-to-Noise Ratio on the Observation Time

We will take a look at a simple example, before going into a general discussion. Let us consider the throwing of a perfect hexahedral die. Each throwing is independent, so the probabilities of the numbers of pips are equal to 1/6 as shown in Figure 2-15(a). If two identical dice are thrown at a time, then the probabilities of the average number of pips are shown in Figure 2-15(b). It can be seen that, in the case of throwing two dice, the probabilities of the average number of pips are more centrally distributed about the mean than those when one die is thrown at a time.

In the analogy to the throwing of two dice, let us consider the average of the positions of T balls, when T balls are released in the Galton board. The variance of the

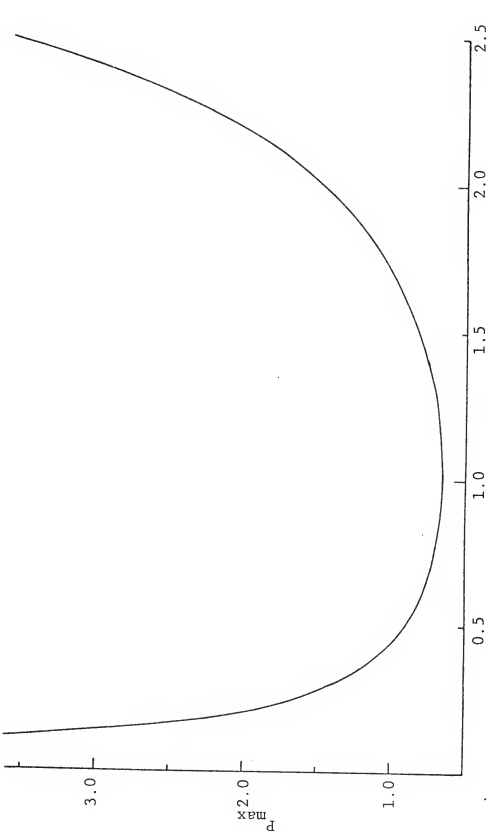

Fig. 2-14 - The Maximum Probability Density

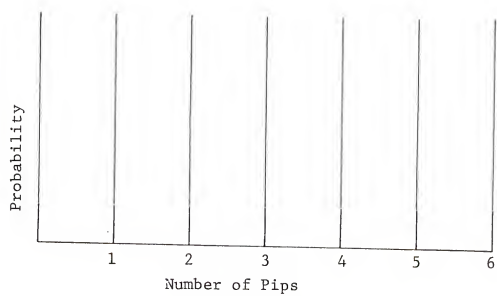

(a)

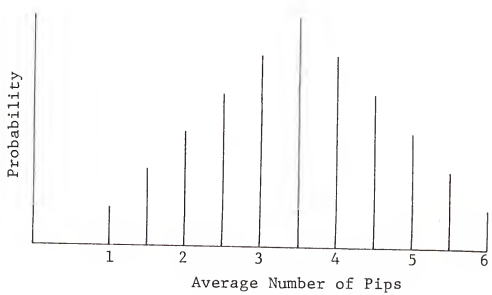

(b)

Fig. 2-15 - The Probability of (a) Throwing one Die
(b) Throwing two Dice

average of the positions of T balls, n_T, is

$$n_T = \frac{n}{T} \tag{2-50}$$

Therefore, the probability, $P_T(N)$, is approximately given by

$$P_T(N) = \frac{1}{\sqrt{2\pi n_T}} \exp\left(-\frac{N^2}{2n_T}\right)$$

$$= \frac{\sqrt{T}}{\sqrt{2\pi n}} \exp\left(-\frac{TN^2}{2n}\right) \tag{2-51}$$

If the observation time of the detector is increased T time, the probability density function, $P_T(I)$, is approximately given by

$$P_T(I) = P_T(N) \left|\frac{dN}{dI}\right|$$

$$= \frac{\sqrt{T}}{\sqrt{2\pi}\ \beta\ I} \exp\left[-\frac{T}{2\beta^2} \ln^2 \left(\frac{I}{I_{oT}}\right)\right] \tag{2-52}$$

where I_{oT} is the geometric mean of the transmitted irradiances. The signal-to-noise ratio, S/N, when the observation time is increased T times, is

$$\frac{S}{N} = \left[\exp\left(\frac{\beta^2}{T}\right) - 1\right]^{-\frac{1}{2}} \tag{2-53}$$

Equation (2-53) is plotted in Figure 2-16. When T is sufficiently large, then

$$\frac{S}{N} = \frac{\sqrt{T}}{\beta} \tag{2-54}$$

From Equations (2-40), (2-41) and (2-52) the probability density function, $P_T(I)$, approaches a normal function as T increases, because $\beta/\sqrt{T}$ becomes smaller.

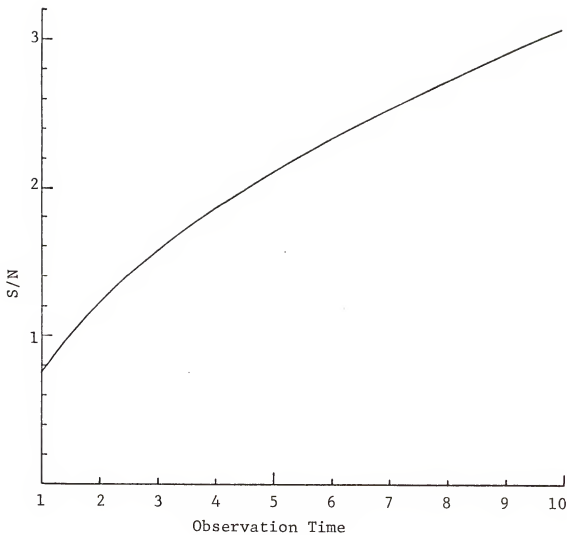

Fig. 2-16 - Dependence of Signal-To-Noise Ratio on the Observation Time (β = 1)

As the observation time increases T times, the average irradiance should remain the same, i.e.,

$$\int_0^\infty I\, P_T(I)\, dI = \int_0^\infty I\, P(I)\, dI \tag{2-55}$$

or

$$I_{oT} \exp\left(\frac{\beta^2}{2T}\right) = I_o \exp\left(\frac{\beta^2}{2}\right) \tag{2-56}$$

then

$$I_{oT} = I_o \exp\left(\frac{\beta^2}{2} - \frac{\beta^2}{2T}\right) \tag{2-57}$$

The most probable irradiance, $I_{T,\ max}$, when the observation time increases, derived from

$$\frac{dP_T(I)}{dI} = 0 \tag{2-58}$$

is given by

$$I_{T,\ max} = I_{oT} \exp\left(-\frac{\beta^2}{T}\right)$$

$$= I_o \exp\left(\frac{\beta^2}{2} - \frac{3\beta^2}{2T}\right) \tag{2-59}$$

Dependence of the Signal-to-Noise Ratio on the Aperture

Similarly, when the observation time is increased T times and the aperture is increased W times, and if the source is homogeneous and bigger than the aperture, then the probability density function of the transmitted irradiances

$$P_{TW}(I) = \frac{\sqrt{TW}}{\sqrt{2\pi}\ \beta\ I} \exp\left[-\frac{TW}{2\beta^2}\ \ln^2\left(\frac{I}{I_{oTW}}\right)\right] \tag{2-60}$$

where I_{oTW} is the geometrical mean of the transmitted irradiances given by

$$I_{oTW} = I_o \left(\frac{\beta^2}{2} - \frac{\beta^2}{2TW}\right) \tag{2-61}$$

The signal-to-noise ratio is

$$\frac{S}{N} = \left[\exp\left(\frac{\beta^2}{TW}\right) - 1\right]^{-\frac{1}{2}} \tag{2-62}$$

When T or W is sufficiently large, we have

$$\frac{S}{N} = \frac{\sqrt{TW}}{\beta} \tag{2-63}$$

From the above equation, we see that the signal-to-noise ratio is proportional to the square root of the observation time or the aperture.

CHAPTER III
THE LOGNORMAL APPROACH TO SHOT NOISE

In the previous chapter, only the noise caused by the randomness of the medium was considered. In this chapter, the noise due to the nature of photons caused by the light passing through a homogeneous medium is considered.

Bernoulli's Distribution[133,134]

The consideration here is that the medium is homogeneous with a transmittance, t_m, and that a photon counter is employed with a quantum efficiency, η. Therefore, the probability of a single photon, p, passing through the medium and being detected is given by

$$p = t_m \eta \tag{3-1}$$

The probability of x photons being detected by the photon counter, $P_m(x)$, when m photons are emitted from a stable light source and are travelling toward the detector through the homogeneous medium is given by

$$P_m(x) = \frac{m!}{x!(m - x)!} p^x (1 - p)^{m-x} \tag{3-2}$$

and the expected (or average) number of photons being detected by the detector, E(x), is[135]

$$E(x) = m\,p \tag{3-3}$$

Also, the standard deviation of the numbers of the detected photons is

$$\sigma_x = \sqrt{mp(1 - p)} \tag{3-4}$$

When m is sufficiently large, it can be shown that Equation (3-2) becomes asymptotically[136]

$$P_m(x) = \frac{1}{\sqrt{2\pi}\sqrt{mp(1 - p)}} \exp\left[-\frac{(x - mp)^2}{2mp(1 - p)}\right] \tag{3-5}$$

If x is treated as a continuous variable, we have approximately

$$E(x) = mp \tag{3-6}$$

and

$$\sigma_x = \sqrt{mp(1 - p)} \tag{3-7}$$

The approximation is pretty good for small m (≥ 5), as long as p is not too far from 1/2. When m is very large and p is very small, Equation (3-2) approaches the Poisson distribution given by [137-139]

$$P_m(x) = \frac{(mp)^x}{x!} \exp(-mp) \tag{3-8}$$

with mean

$$E(x) = mp \tag{3-9}$$

and standard deviation

$$\sigma_x = \sqrt{mp} \tag{3-10}$$

When n is extremely large, Equation (3-8) approaches the normal distribution

$$P_m(x) = \frac{1}{\sqrt{2\pi}\sqrt{mp}} \exp\left[-\frac{(x - mp)}{2mp}\right] \tag{3-11}$$

and the mean and the standard deviation remain the same.[137,138]

Bernoulli's distribution, given by Equation (3-2), is very tedious for calculation and manipulation. The normal distribution, given by Equation (3-5), is very convenient for calculation, but for small p it does not have the asymmetry of distribution. Poissonian distribution, given by Equation (3-8), has the asymmetry of distribution and is less tedious than Bernoulli's distribution, but it is still inconvenient for calculation and manipulation, because of the factorial term in it. An approximate expression for Bernoulli's distribution will be given for having both the asymmetry and the convenience of calculation.

Lognormal Approximation to Bernoulli's Distribution

When m is very large, Stirling's formula is given by[139]

$$\ln m! \doteq m \ln m - m + \ln \sqrt{2\pi m} \tag{3-12}$$

Equation (3-2) and Stirling's formula, when both m and x are very large, become

$$\ln P_m(x) \doteq -x \ln \frac{x}{mp} - (m - x) \ln \frac{m - x}{m(1 - p)} + \tfrac{1}{2} \ln \frac{m}{2\pi x(m - x)} \tag{3-13}$$

Let us define a parameter, u given by

$$\frac{x}{mp} \exp\left(\frac{q}{2mp}\right) = \left\{\frac{1 + u\sqrt{\frac{q}{mp}}}{1 - u\sqrt{\frac{q}{mp}}}\right\}^{\frac{1}{2}} \tag{3-14}$$

where q = 1 - p.

When m is very large, Equation (3-14) becomes

$$\frac{x}{mp} \doteq 1 + u\sqrt{\frac{q}{mp}} \tag{3-15}$$

and we have

$$\ln \frac{x}{mp} \doteq \ln \left(1 + u\sqrt{\frac{q}{mp}}\right)$$

$$\doteq u\sqrt{\frac{q}{mp}} - \frac{u^2 q}{2mp} \tag{3-16}$$

From Equations (3-15) and (3-16),

$$x \ln \frac{x}{mp} \doteq u\sqrt{mpq} - \frac{1}{2} u^2 q \tag{3-17}$$

From Equation (3-15),

$$m - x \doteq mq - u\sqrt{mpq} \tag{3-18}$$

so,

$$\ln \frac{m - x}{mq} \doteq \ln \left(1 - u\sqrt{\frac{p}{mq}}\right)$$

$$\doteq - u\sqrt{\frac{p}{mq}} - \frac{u^2 p}{2mq} \tag{3-19}$$

then,

$$(m - x) \ln \frac{m - x}{mq} \doteq - u\sqrt{mpq} - \frac{1}{2} u^2 p \tag{3-20}$$

Substituting Equations (3-17) and (3-20) into Equation (3-13) yields

$$\ln P_m(x) = - \frac{u^2}{2} + \frac{1}{2} \ln \frac{m}{2\pi x(m - x)} \tag{3-21}$$

Therefore,

$$P_m(x) \doteq \sqrt{\frac{m}{2\pi x(m - x)}} \exp\left(- \frac{u^2}{2}\right) = \frac{1}{x}\sqrt{\frac{mx}{2\pi(m - x)}} \exp\left(- \frac{u^2}{2}\right)$$

$$\doteq \frac{1}{x}\sqrt{\frac{mp}{2\pi q}}\ \exp\left(-\frac{u^2}{2}\right) \tag{3-22}$$

Taking logarithms on Equation (3-14) yields

$$\ln\{\frac{x}{mp}\exp\left(\frac{q}{2mp}\right)\} = \frac{1}{2}\ln\frac{1+u\frac{q}{mp}}{1-u\frac{q}{mp}}$$

$$\doteq u\sqrt{\frac{q}{mp}} \tag{3-23}$$

Cancelling u in Equations (3-22) and (3-23) gives

$$P_m(x) = \sqrt{\frac{mp}{2\pi q}}\ \frac{1}{x}\exp\{-\frac{mp}{2q}\ln^2\ \frac{1}{mp\exp\left(-\frac{q}{2mp}\right)}\} \tag{3-24}$$

It can be seen that mp exp (- q/2mp) is the teometrical mean of x in the above equation. To treat the distribution of transmitted irradiances passing through a turbulent medium when the nature of photons is also considered, Equations (2-60) and (3-24) should be used in the Mandel formula.[122]

From Equation (3-24), when m is very large, the mean and standard deviation, respectively, are given by

$$E(x) = mp \tag{3-25}$$

and

$$\sigma_x = mp\{\exp\left(\frac{q}{mp}\right) - 1\}^{-\frac{1}{2}} \tag{3-26}$$

When m is very large,

$$\sigma_x = \sqrt{mpq} = \sqrt{E(x)q} \tag{3-27}$$

When p is very small, the signal-to-noise ratio, S/N, is given by

$$\frac{S}{N} = \frac{E(x)}{\sigma_x} = \sqrt{mp} = \sqrt{E(x)} \qquad (3\text{-}28)$$

When p is small, and m is extremely large, Equation (3-24) becomes

$$P_m(x) = \frac{1}{\sqrt{2\pi mp}} \exp\{-\frac{(x - mp)^2}{2mp}\} \qquad (3\text{-}29)$$

Thus, the four distributions, Bernoulli's, the normal, Poissonian and the lognormal are related. The lognormal distribution has the advantage of Bernoulli's and Poissonian distributions and that of the normal distribution, i.e., the skewedness and the convenience in calculation, respectively.

In the previous chapter (Chapter II), the signal-to-noise is independent of the source irradiance in a random medium. In this chapter, the nature of photons has been taken into consideration in a homogeneous medium, and the result derived is that the signal-to-noise ratio increases as the source irradiance increases.

CHAPTER IV
THE LOGNORMAL EMISSION PROFILE

Gaussian Doppler Profile[140-145]

According to the principles of special relativity, when a light source is approaching an observer, the expression for the Doppler shift of frequency is given by

$$\frac{\nu}{\nu_o} = \frac{\sqrt{(1 + \frac{v_x}{c})}}{\sqrt{(1 - \frac{v_x}{c})}} \qquad (4\text{-}1)$$

where ν is the observed frequency of the radiation from a light source which approaches the observer with a velocity along the direction of the sight, v_x, ν_o is the observed frequency of the radiation of the light source when it is at rest, and c is the velocity of light for a medium with refractive index of unity.[140]

When $v_x << c$, Equation (4-1) becomes

$$\frac{\nu}{\nu_o} = (1 + \frac{v_x}{c}) \qquad (4\text{-}2)$$

or

$$\frac{\lambda}{\lambda_o} = (1 - \frac{v_x}{c}) \qquad (4\text{-}3)$$

where λ and λ_o are the observed wavelengths of the radiating

source in motion and at rest, respectively. If the light source is receding from the observer, one merely changes the sign of the velocity, v_x, in Equation (4-1), (4-2), or (4-3). The expression for the Doppler profile can be obtained from Equations (4-2) and (4-3), and the Maxwellian distribution of the kinetic velocities along the sight, $P(v_x)$, given by

$$P(v_x) = \left(\frac{m}{2\pi kT}\right)^{\frac{1}{2}} \exp\left(-\frac{mv_x^2}{2kT}\right) \qquad (4\text{-}4)$$

where m is the mass of the emitting particle, k is the Boltzmann constant, and T is the absolute temperature of the medium.[141] Therefore, the expression for the Doppler profile, $P(\nu)$ or $P(\lambda)$, on the scale of frequency or wavelength, respectively, is given by

$$P(\nu) = P(v_x)\left|\frac{dv_x}{d\nu}\right| = \left(\frac{mc^2}{2\pi kT\nu_o^2}\right)^{\frac{1}{2}} \exp\left\{-\frac{mc^2}{2kT\nu_o^2}(\nu - \nu_o)^2\right\} \qquad (4\text{-}5)$$

or

$$P(\lambda) = P(v_x)\left|\frac{dv_x}{d\lambda}\right| = \left(\frac{mc^2}{2\pi kT\lambda_o^2}\right)^{\frac{1}{2}} \exp\left\{-\frac{mc^2}{2kT\lambda_o^2}(\lambda - \lambda_o)^2\right\} \qquad (4\text{-}6)$$

Equation (4-5) or (4-6) shows that the Doppler emission profile is symmetric about the mean. However, careful experimental studies of the emission profiles showed that they were not symmetrical.[143] Integrating Equations (4-5) and (4-6) for ν and λ from $-\infty$ to ∞, respectively, gives

$$\int_{-\infty}^{\infty} P(\nu)\, d\nu = 1 \qquad (4\text{-}7)$$

and

$$\int_{-\infty}^{\infty} P(\lambda)\, d\lambda = 1 \qquad (4\text{-}8)$$

Equation (4-7) or (4-8) indicates that the probability of photons, emitted from the sources with the thermal motions, distributed in the range for ν or λ from $-\infty$ to ∞, respectively, is unity. But "negative wave numbers" (frequencies or wavelengths) "have no physical reality."[144] If the integration is done in the interval from 0 to ∞ for ν or λ, in accordance with the physical reality, then the probability is less than unity which is against the physical reality. Hence, the average energy of emitted photons, E_{ave}, calculated from Equation (4-5) or (4-6), is given by

$$E_{ave} = \int_{0}^{\infty} h\, P(\nu)\, d\nu > h\nu_o \qquad (4\text{-}9)$$

or

$$E_{ave} = \int_{0}^{\infty} \frac{hc}{\lambda} P(\lambda)\, d\lambda = \infty > \frac{hc}{\lambda_o} \qquad (4\text{-}10)$$

It is interesting to note that (i) the average energy of the photons emitted from sources with thermal motions is greater than the average energy of photons emitted from sources at rest, $h\nu_o$ or hc/λ_o, as shown in Equation (4-9) or (4-10) respectively, and (ii) the emission profile in terms of the wavelength as shown in Equation (4-10) is unreasonable.

The half-widths of the Doppler broadenings derived from Equations (4-5) and (4-6) are given by[145]

$$\Delta\nu_D = \frac{2\nu_o}{c} \left(\frac{2kT \ln 2}{m}\right)^{\frac{1}{2}} \qquad (4\text{-}11)$$

and

$$\Delta\lambda_D = \frac{2\lambda_o}{c}\left(\frac{2kT \ln 2}{m}\right)^{\frac{1}{2}} \qquad (4\text{-}12)$$

Lognormal Hypothesis

The hypothesis is based upon the following reasons:

(i) In spectroscopy, both frequency and wavelength are positive quantities. Similarly, variables are positive in the lognormal distribution as shown in Equation (2-35).

(ii) In the emission profile, the width of a spectral line is proportional to the mean value (frequency or wavelength) as shown in Equation (4-11) or (4-12). Similarly, in the lognormal distribution, the standard deviation is proportional to the mean as shown in Equation (2-39). In the normal distribution, the standard deviation and the mean should be statistically independent.[146]

(iii) In the emission profile, the expected energy of a random system is greater than the expected energy of a homogeneous system as shown in Equations (4-9) and (4-10). Similarly, in the lognormal distribution, the expected value of a variable in a random system is greater than the expected value of a variable in a homogeneous system, as shown in Equation (2-38).

Hence, it would be reasonable to assume that the Doppler profile would take a lognormal shape, given by

$$P(\nu) = \frac{1}{\sqrt{2\pi}\ \beta_D \nu} \exp\left(-\frac{1}{2\beta_D^2} \ln^2 \frac{\nu}{\nu_o}\right) \tag{4-13}$$

or

$$P(\lambda) = \frac{1}{\sqrt{2\pi}\ \beta_D \lambda} \exp\left(-\frac{1}{2\beta_D^2} \ln^2 \frac{\lambda}{\lambda_o}\right) \tag{4-14}$$

where β_D is a dispersion parameter for the spectral broadening due to the thermal randomness.

The probability of photons emitted from sources experiencing thermal motions, in the range from 0 to ∞, for ν or λ, is given by

$$\int_0^\infty P(\nu)\, d\nu = 1 \tag{4-15}$$

or

$$\int_0^\infty P(\lambda)\, d\lambda = 1 \tag{4-16}$$

The average energy of photons from sources experiencing thermal motion, E_{ave}, obtained from Equation (4-13) or (4-14) is given by, respectively,

$$E_{ave} = \int_0^\infty h\nu P(\nu)\, d\nu = h\nu_o \exp\left(\frac{\beta_D^2}{2}\right) \tag{4-17}$$

or

$$E_{ave} = \int_0^\infty \frac{hc}{\lambda} P(\lambda)\, d\lambda = \frac{hc}{\lambda_o} \exp\left(\frac{\beta_D^2}{2}\right) \tag{4-18}$$

It is seen from the above expressions, that the average energy of photons from the sources experiencing thermal motions is greater than that of photons from the sources at rest. A discussion will be given to understand where the excess energy comes from in the above expressions and to evaluate β_D.

We can consider that half of the emitting particles are moving toward the observer and the other half of the emitting particles are receding from the observer with the root-mean-square velocities $\bar{v}_x$ and $-\bar{v}_x$, respectively, which are given by

$$\frac{1}{2} m \bar{v}_x^2 = \frac{1}{2} kT \tag{4-19}$$

The average energy of photons given off by the emitting particles, E_{ave}, from Equation (4-1), is given by

$$E_{ave} = h\nu = \frac{1}{2} h\nu_o \left[\left(\frac{1 + \frac{\bar{v}_x}{c}}{1 - \frac{\bar{v}_x}{c}}\right)^{\frac{1}{2}} + \left(\frac{1 - \frac{\bar{v}_x}{c}}{1 + \frac{\bar{v}_x}{c}}\right)^{\frac{1}{2}} \right]$$

$$= h\nu_o \left(1 - \frac{\bar{v}_x^2}{c^2}\right)^{-\frac{1}{2}} \tag{4-20}$$

The above equation indicates that the average energy of photons from the sources experiencing thermal motions, E_{ave}, is greater than that of photons from the sources at rest, $h\nu_o$.

Substituting Equation (4-20) into Equation (4-17) or (4-18),

$$\exp\left(\frac{d_D^2}{2}\right) = \left(1 - \frac{\bar{v}_x^2}{c^2}\right)^{-\frac{1}{2}} \tag{4-21}$$

and taking logarithms on both sides of the above equation yields

$$d_D^2 = - \ln \left[1 - \frac{\bar{v}_x^2}{c^2}\right] \tag{4-22}$$

For $\bar{v}_x << c^2$, in the analytical laboratory, then the above equation becomes

$$\beta_D^2 = (\frac{\bar{v}_x}{c})^2 \qquad (4\text{-}23)$$

Substituting Equation (4-19) into the above equation gives

$$\beta_D^2 = \frac{kT}{mc^2} \qquad (4\text{-}24)$$

Substituting Equation (4-24) into Equations (4-13) and (4-14) gives

$$P(\nu) = (\frac{mc^2}{2\pi kT\nu^2})^{\frac{1}{2}} \exp\ [-\frac{mc^2}{2kT} \ln^2 \frac{\nu}{\nu_o}] \qquad (4\text{-}25)$$

and

$$P(\lambda) = (\frac{mc^2}{2\pi kT\lambda^2})^{\frac{1}{2}} \exp\ [-\frac{mc^2}{2kT} \ln^2 \frac{\lambda}{\lambda_o}] \qquad (4\text{-}26)$$

The above equations show that the Doppler emission profiles are not symmetric and the integrations for ν and λ from 0 to ∞ are unity. It has been shown that the lognormal distribution, Equation (2-35), is approximated by the normal distribution, Equation (2-42), for small values of β^2. Similarly, the log-normal Doppler emission profile, Equation (4-25) or (4-26), can be approximated by the normal Doppler emission profile, Equation (4-5) or (4-6), for small values of kT/mc^2. The asymmetry and the peakedness of the lognormal Doppler emission profile, Equation (4-25) or (4-26), can be easily calculated from Equations (2-40) and (2-21), respectively.

So far, the advantages of the lognormal expressions over the Gaussian expressions have been shown. The mathematical validity of the lognormal expression will be given in the next chapter to show that the Equations (4-25) and (4-26) are more accurate than Equations (4-5) and (4-6).

Lorentzian Profile

Another major cause of line broadening in a gas results from collisions of radiating particles (atoms, ions or molecules) with each other. The following expression describes the frequency distribution of collision-broadened (Lorenthian) line

$$P(\nu) = \left(\frac{\Delta\nu}{2\pi}\right) \frac{1}{(\nu - \nu_o)^2 + \left(\frac{\Delta\nu}{2}\right)^2} \qquad (4\text{-}27)$$

where ν_o is the center frequency, and $\Delta\nu$ is the width between the half-power points of the curve.[147]

The integration

$$\int_0^\infty P(\nu)\, d\nu < \int_{-\infty}^{\infty} P(\nu)\, d\nu = 1 \qquad (4\text{-}28)$$

indicates that the probability of a photon distributed in the range, ν from 0 to ∞, is less than unity. The average energy emitted from a Lorentzian line, given by

$$E_{ave} = \int_0^\infty h\nu\, P(\nu)\, d\nu = \infty \qquad (4\text{-}29)$$

is not well defined, because the integration is divergent.[148] Beside the conflicts to the physical reality, the Lorentzian line cannot explain the shift and asymmetry of the line profile. It can only describe that the line profile is more peaked than the Gaussian profile.

Lognormal Shape of Doppler-Collisional Broadening

Assuming that the Doppler broadening and the collisional broadening are two independent processes, the profile for the Doppler-collisional broadening, $P(\nu)$, is given by

$$P(\nu) = \frac{1}{\sqrt{2\pi}\beta\nu} \exp\left(-\frac{1}{2\beta^2} \ln^2 \frac{\nu}{\nu_{os}}\right) \tag{4-30}$$

where

$$\beta^2 = \beta_D^2 + \beta_C^2 \tag{4-31}$$

and β_C is the dispersion parameter of the spectral profile due to the collisional process, and ν_{os} is the geometrical mean of the frequencies.

Assuming the energy of the system of interest remains unchanged due to the collisional process, the average energy, emitted from a Doppler-collisional profile, is given by

$$E_{ave} = \int_0^\infty h\nu \, P(\nu) \, d\nu$$

$$= h\nu_{os} \exp\left(\frac{1}{2}\beta_D^2 + \frac{1}{2}\beta_C^2\right) \tag{4-32}$$

Equations (4-17) and (4-32) give

$$\nu_{os} = \nu_o \exp\left(-\frac{1}{2}\beta_C^2\right) \tag{4-33}$$

Similarly, the Doppler-collisional profile in terms of wavelength is given by

$$P(\lambda) = \frac{1}{\sqrt{2\pi}\beta\lambda} \exp\left(-\frac{1}{2\beta^2} \ln^2 \frac{\lambda}{\lambda_{os}}\right) \tag{4-34}$$

where λ_{os} is the geometrical mean of the wavelengths,

given by

$$\lambda_{os} = \lambda_o \exp\left(\frac{1}{2}\beta_C^2\right) \tag{4-35}$$

Because the reliable interpretations of the shifts in the spectral profiles were mostly done with the absorption method, hence the shifts of the spectral profiles will be discussed in Chapter VI.

CHAPTER V
THE DOPPLER EFFECT AND THE DISTRIBUTION OF VELOCITIES

In this chapter, an approximate expression for the Doppler effect is discussed. The lognormal distribution of emission profile is also derived from the approximate expression of the Doppler effect with mathematical validity. The distributions of thermal velocities are also easily derived from the lognormal distribution of emission profile without the concept of phase space being involved.

Approximate Expression for Doppler Effect

It is assumed that the approximate expression for the Doppler effect is given by

$$\ln \frac{\nu}{\nu_o} = \frac{v_x}{c} \tag{5-1}$$

or

$$\frac{\nu}{\nu_o} = \exp\left(\frac{v_x}{c}\right) \tag{5-2}$$

When $v_x \ll c$, expanding the above equation yields

$$\frac{\nu}{\nu_o} = 1 + \frac{v_x}{c} + \frac{1}{2}\frac{v_x^2}{c^2} \tag{5-3}$$

The polynomial expansion of Equation (4-1), derived from the principles of relativity, when $v_x << c$, is

$$\frac{\nu}{\nu_o} = 1 + \frac{v_x}{c} + \frac{1}{2}\frac{v_x^2}{c^2} \qquad (5\text{-}4)$$

It is seen from Equations (5-3) and (5-4) that the Equation (5-1) is more accurate than the Equation (4-2)

$$\frac{\nu}{\nu_o} = 1 + \frac{v_x}{c}$$

Equation (5-1) and the Maxwell distribution of one-dimensional velocitied of Equation (4-4) give

$$P(\nu) = \frac{1}{\sqrt{2\pi}\beta\nu} \exp\left(-\frac{1}{2\beta^2} \ln^2 \frac{\nu}{\nu_o}\right) \qquad (5\text{-}5)$$

where $\beta = (kT/mc^2)^{\frac{1}{2}}$.

The above equation is identical with Equation (4-25), which is derived from the lognormal assumption.

It is concluded that the lognormal expression for the Doppler profile, Equation (4-25), is more valid than Gaussian expression, Equation (4-13), because Equation (5-1) suffers less approximation than Equation (4-2).

The Distribution of Velocities

In the studies of plasmas, the flux of particles reaching the electrodes has been represented by three different expressions for the same thermal velocity in treating the same problem.[149-151] Considerations should be based upon the dis-

tributions of velocities. The mathematical derivations for the distributions of velocities are quite complicated. However they can be easily derived from the lognormal approach.

The one-dimensional distribution of velocities, $P(v_x)$, can be easily derived, from the lognormal Doppler profile, in Equation (4-25), and the Doppler effect, in Equation (5-1), and is given by

$$P(v_x) = P(\nu)\left|\frac{d\nu}{dv_x}\right|$$

$$= \left(\frac{m}{2\pi kT}\right)^{\frac{1}{2}} \exp\left(-\frac{mv_x^2}{2kT}\right) \qquad (5\text{-}6)$$

The two-dimensional distribution of velocities, which is defined as two one-dimensional distributions of velocities in x and y directions, sometimes called the circular normal of Rayleigh distribution, can be easily derived as

$$P(v_2) = \frac{v_2}{\beta^2} \exp\left(-\frac{v_2^2}{\beta^2}\right) \qquad (5\text{-}7)$$

where $\beta = (kT/mc^2)^{\frac{1}{2}}$, $v_2 = (v_x^2 + v_y^2)^{\frac{1}{2}}$ and v_y is the velocity of the particle along the y-axis.[13,152]

The three-dimensional distribution of velocities in x, y and z directions, sometimes called the sperical normal or Maxwell distribution, can be easily derived as

$$P(v_3) = \frac{\sqrt{2}}{\sqrt{\pi}} \left(\frac{v_3^2}{\beta^2}\right) \exp\left(\frac{v_3^2}{2\beta^2}\right) \qquad (5\text{-}8)$$

where $\beta = (kT/mc^2)^{\frac{1}{2}}$, $v_3 = (v_x^2 + v_y^2 + v_z^2)^{\frac{1}{2}}$ and v_z is the velocity of the particle along the z-axis.[13,152]

CHAPTER VI
LOGNORMAL ABSORPTION PROFILES

Introduction

In an actual absorption experiment, the intensity of light transmitted through a fixed layer of material is recorded while the frequency of the incident light is varied. From the assumption that the decrease of the light intensity, I, on passage through material of thickness, dx, is proportional to I dx, it is inferred that the variation of I with depth x follows the law

$$I_\nu(x) = I_\nu(0) \exp(-k_\nu x) \qquad (6\text{-}1)$$

where $I_\nu(0)$ is the incident intensity at frequency ν (Hz) and k_ν (cm^{-1}) is called absorption coefficient at frequency ν.[147]

In order to evaluate k_ν quantitatively, it is advisable to take a look at the process of absorption.[147] Consider a parallel beam of light of frequency between ν and $\nu + d\nu$ and intensity I_ν travelling in the positive x-direction through a layer of atoms bounded by the planes x and x + dx. For simplicity, let the refractive index of this medium be unity, and the velocity of light be c. The phase front will travel through the slab of thickness dx in the time dt = dx/c. Suppose there are N_1 atoms/cm^3 in level 1, of which $dN_{1\nu}$ are

capable of absorbing the incident radiation and $dN_{2\nu}$ excited atoms capable of emitting the same frequency radiation. Neglecting the effect of spontaneous re-emission in view of the fact that it occurs equally in all directions, the decrease in energy of the incident beam is given by

$$-d(I_\nu d\nu) = h\nu(B_{12}dN_{1\nu} - B_{21}dN_{2\nu})I\,\frac{dx}{\nu c} \qquad (6\text{-}2)$$

where B_{12} is the coefficient of stimulated absorption for the transition from level 1 to level 2 and B_{21} is the coefficient of stimulated emission for the transition from level 2 to level 1.

From the above equation, it follows that

$$-\frac{1}{I_\nu}\frac{dI_\nu}{dx}\,d\nu = \frac{h\nu}{c}\,(B_{12}dN_{1\nu} - B_{21}dN_{2\nu}) \qquad (6\text{-}3)$$

Recognizing that the left-hand member is $k_\nu d\nu$ as defined by Equation (6-1), the above equation becomes

$$k_\nu d\nu = \frac{h\nu}{c}\,(B_{12}dN_{1\nu} - B_{21}dN_{2\nu}) \qquad (6\text{-}4)$$

Assuming that coefficients B_{12} and B_{21} are independent of frequency, then integrating over the entire absorption line yields approximately

$$\int_0^\infty k_\nu d\nu \doteq \int_{-\infty}^{\infty} k_\nu d\nu = \frac{h\nu_o}{c}\,(B_{12}N_1 - B_{21}N_2) \qquad (6\text{-}5)$$

where ν_o is the frequency at the center of the line, assuming that the atoms are normally distributed about ν_o. When the

stimulated emission is ignored, then the above equation becomes

$$\int_0^\infty k_\nu d\nu = \frac{h\nu_o}{c} B_{12}N_1 \qquad (6\text{-}6)$$

A better integration of Equation (6-4), assuming that the stimulated coefficients are independent of frequency and that the stimulated emission is negligible, is given by[153]

$$\int_0^\infty \frac{k_\nu}{\nu} d\nu = \frac{h}{c} B_{12}N_1 \qquad (6\text{-}7)$$

For the atomic line, Equation (6-6) is a good approximation of Equation (6-7).[154] However for the molecular band, Equation (6-7) is favorable.[155]

Lognormal Absorption Profile

Assuming that the distribution of photons follows the lognormal model, as shown by Equation (4-30), we have

$$dN_{1\nu} = N_1 P(\nu)d\nu \qquad (6\text{-}8)$$

Assuming that the stimulated emission is negligible, and substituting the above equation into Equation (6-4) yields

$$k_\nu = \frac{h\nu}{c} B_{12}N_1P(\nu) \qquad (6\text{-}9)$$

Using the relation

$$B_{12} = \frac{\pi e^2}{m_e h\nu} f$$

where e and m_e are the charge and the mass of the electron, respectively, and f is the oscillator strength between level 1 and level 2, then Equation (6-9) becomes

$$k_\nu = \frac{\pi e^2}{m_e c} N_1 f \frac{1}{\sqrt{2\pi}\beta\nu} \exp\left(-\frac{1}{2\beta^2} \ln^2 \frac{\nu}{\nu_{os}}\right) \tag{6-11}$$

Integrating the above equation, assuming f is constant, because oscillator strength is dimensionless, yields

$$\int_0^\infty k_\nu d\nu = \frac{\pi e^2}{m_e c} N_1 f \tag{6-12}$$

Defining ν_{max} as the frequency where k_ν is maximum, as

$$\frac{dk_\nu}{d\nu} = 0 \tag{6-13}$$

From Equation (4-33), the above equation gives

$$\nu_{max} = \nu_o \exp\left(-\beta_D^2 - \frac{3}{2}\beta_C^2\right) \tag{6-14}$$

The above equation indicates that both the Doppler and collisional effects will cause a red-shift of the absorption line. Ignoring the slit function of a grating monochromator when the slit is very narrow, then

$$k_\lambda = k_\nu$$

$$= \frac{\pi e^2}{m_e c} N_1 f \left(\frac{\lambda}{\sqrt{2\pi}\beta c}\right) \exp\left(-\frac{1}{2\beta^2} \ln^2 \frac{\lambda}{\lambda_{os}}\right) \tag{6-15}$$

Integrating the above equation yields

$$\int_0^\infty k_\lambda d\lambda = \frac{e^2}{m_e c^2} N_1 f \lambda_o^2 \exp\left(\frac{1}{2}\beta_D^2 + \beta_C^2\right) \tag{6-16}$$

The above equation indicates that the absorption integral (or integrated absorption coefficient) increases with increasing β_D and β_C. Defining λ_{max} as the wavelength where k_λ is maximum as

$$\frac{dk_\lambda}{d\lambda} = 0 \qquad (6\text{-}17)$$

then

$$\lambda_{max} = \lambda_o \exp\left(\beta_D^2 + \frac{3}{2}\beta_C^2\right) \qquad (6\text{-}18)$$

The above equation indicates that both the Doppler and collisional effects will cause a red-shift of an absorption line. Because Equation (6-4) is valid for molecular bands, assuming β_C increases with increasing temperature, one will expect the experimental result showing a red-shift of molecular absorption bands in the gaseous phase, when temperature becomes higher.[156]

Both the temperature and the collision will affect the emission and the absorption profiles, as shown in Equations (6-11) and (6-15). Hence, for example, in the atomic fluorescence spectroscopy with a line source, the fluorescence signal or the quantum yield of an excitation process will be different if the temperature is changed, or if the collisional effect is changed, even if there is not collisional excitation or de-excitation.

Lognormal and Lorentzian Absorption Profiles

It will be shown here that the lognormal absorption profiles can be approximated by the Lorentzian absorption profiles.

The Lorentzian absorption profiles, with frequency and wavelength scales, respectively, are given by

$$k_\nu = k_o \frac{\Delta\nu^2}{4(\nu - \nu_o)^2 + \Delta\nu^2} \tag{6-19}$$

and

$$k_\lambda = k_o \frac{\Delta\lambda^2}{4(\lambda - \lambda_o)^2 + \Delta\lambda^2} \tag{6-20}$$

where k_o (cm^{-1}) is the value of k_ν (cm^{-1}) or k_λ (cm^{-1}) at $\nu = \nu_o$ or $\lambda = \lambda_o$, respectively, and $\Delta\nu$ or $\Delta\lambda$ is the half-width of the Lorentzian absorption profile, Equation (6-19) or (6-20), respectively.[157]

Ignoring the small effect of spectral shift in Equation (6-11) gives

$$k_\nu = \left(\frac{\pi e^2}{m_e c}\right) N_1 f \left(\frac{1}{\sqrt{2\pi}\beta\nu}\right) \frac{1}{\exp\left(\frac{1}{2\beta^2} \ln^2 \frac{\nu}{\nu_o}\right)}$$

When ν is in the vicinity of ν_o, the above equation becomes

$$k_\nu \doteq \left(\frac{\pi e^2}{m_e c}\right) N_1 f \left(\frac{1}{\sqrt{2\pi}\beta\nu_o}\right) \frac{1}{1 + \frac{1}{2\beta^2} \ln^2 \frac{\nu}{\nu_o}}$$

$$\doteq \left(\frac{\pi e^2}{m_e c}\right) N_1 f \left(\frac{1}{\sqrt{2\pi}\beta\nu_o}\right) \frac{1}{1 + \frac{(\nu - \nu_o)^2}{2\beta^2 \nu_o^2}}$$

Because $k_\nu = k_o$ at $\nu = \nu_o$, the above equation can be expressed as

$$k_\nu = k_o \frac{8\beta^2\nu_o^2}{4(\nu - \nu_o)^2 + 8\beta^2\nu_o^2}$$

Let $\Delta\nu = 2\sqrt{2}\beta\nu_o$, then the above equation, which is derived from the lognormal absorption profile, Equation (6-11), be-

comes the Lorentzian absorption profile, Equation (6-19) when ν is in the vicinity of ν_o. When ν becomes far from ν_o, Equations (6-11) and (6-19) approach zero. Hence, the lognormal absorption profile, Equation (6-11), is approximated by the Lotentzian profile, Equation (6-19), when written in terms of frequency.

Similarly, when written in terms of wavelength, the lognormal absorption profile, Equation (6-15), can be approximated by the Lorentzian absorption profile, Equation (6-20).

The Lorentzian absorption profiles written in terms of frequency and wavelength units, Equations (6-19) and (6-20), respectively, are symmetric about their maxima. It can be seen that if an absorption profile is symmetric on the frequency scale, then the absorption profile replotted versus wavelength cannot be symmetric, because of the reciprocal relationship between frequency and wavelength. Therefore, the Lorentzian absorption profiles with frequency and wavelength scales, Equations (6-19) and (6-20), cannot both be mathematically valid.

CHAPTER VII
ERRORS IN THE REACTIONS OF FIRST-ORDER

Error of the Average Life-Time

Suppose we have a reaction of first-order given by

$$A \rightarrow x + \cdots\cdots \tag{7-1}$$

then, the reaction rate can be expressed as

$$\frac{d[A]}{dt} = - k[A] \tag{7-2}$$

where [A] is the concentration of the species A (cm^{-3}, M or torr) at time t (s), and k is the first-order rate constant of the reaction (s^{-1}).

Integration of the above equation gives

$$[A] = [A]_i \exp(-kt) \tag{7-3}$$

where $[A]_i$ is the initial concentration of species A.

The average life-time, τ, and the standard deviation of the life-time of species A, σ_τ, can be expressed as[158,159]

$$\tau = \frac{\int_0^\infty t(\frac{d[A]}{dt})\, dt}{\int_0^\infty (\frac{d[A]}{dt})\, dt} \tag{7-4}$$

and

$$\sigma_\tau = \{\frac{\int_0^\infty (t - \tau)^2 (\frac{d[A]}{dt})\, dt}{\int_0^\infty (\frac{d[A]}{dt})\, dt}\}^{\frac{1}{2}} \tag{7-5}$$

Using the formula

$$\int_0^\infty t^n \exp(-st)\, dt = \frac{n!}{s^{n+1}} \tag{7-6}$$

and substituting Equation (7-6) into Equations (7-4) and (7-5), yields[159,160]

$$\tau = \frac{1}{k} \tag{7-7}$$

$$\sigma_\tau = \frac{1}{k} \tag{7-8}$$

From the above equations, the relative errors of the life-time in a first-order reaction is given by

$$\frac{\sigma_\tau}{\tau} = 100\% \tag{7-9}$$

The above equation is used to evaluate the natural broadening of a spectral line where the life-time of an excited atom is equal to the standard deviation of the life-time.[157] Because no reliable measurements of life-time were reported with relative errors of 100%, it is possible that the above equation is only valid for a system consisting of one particle.

For a system consisting of m particles, the relative error of the life-time may be approximately given by

$$\frac{\sigma_{\tau,m}}{\tau_m} = \frac{100}{\sqrt{m}}\ \% \tag{7-10}$$

where τ_m is the average life-time of n particles and $\sigma_{\tau,m}$ is the standard deviation of life-time in a system of n particles. For example, in order to have a relative error less than 1%,

ignoring other instrumental errors, the system of interest should consist of tenthousand particles as a minimum.

Time Dependent Rate Constant

A study in a real example will be considered, as in the thermal decomposition of azoisoprane at 270°C, given by[161]

$$(CH_3)_2CH{=}NCH(CH_3)_2 \rightarrow N_2 + C_6H_{14} \qquad (7\text{-}11)$$

Assuming that the reaction is first-order, the initial pressure of azoisoprane is p_i (torr), and at time t, its pressure becomes p_A (torr), with a decrease of x (torr), then[161]

$$p_A = p_i - x \qquad (7\text{-}12)$$

From the rate equation

$$\frac{dp_A}{dt} = -kp_A \qquad (7\text{-}13)$$

then

$$k = \frac{1}{t} \ln \frac{p_i}{p_i - x} \qquad (7\text{-}14)$$

In the above equation, the partial pressure of azoisoprane is not measurable, only the total pressure, p, is measurable, which is the summation of the three partial pressures given by

$$p = p_A + p_{N_2} + p_{C_6H_{14}} = p_i + x \qquad (7\text{-}15)$$

Cancelling x in Equations (7-14) and (7-15) gives

$$k = \frac{1}{t} \ln \frac{p_i}{2p_i - p} \qquad (7\text{-}16)$$

The experimental results for the reaction in Equation (7-11) are duplicated in Table 7-1.[161] It is interesting to see that the calculated rate constant decreases with increasing time. In order to explain this, a new model is proposed here. In this model, it is assumed that, due to some unknown parameters, e.g., the microscopic inhomogeneity of the temperature, the distribution of the rate constant, P(k), follows the normal law, given by

$$P(k) = \frac{1}{\sqrt{2\pi}\beta} \exp\left[-\frac{1}{2\beta^2}(k - k_o)^2\right] \qquad (7\text{-}17)$$

where β is the dispersion parameter (s^{-1}) of the rate constant due to the microscopic inhomogeneity of the rate constant and k_o is the theoretical rate constant or the macroscopic average of the rate constants.

If the rate constant is microscopically homogeneous, the theoretical total pressure, p_o, at time, t, is given by

$$k_o = \frac{1}{t} \ln \frac{p_i}{2p_i - p_o} \qquad (7\text{-}18)$$

From Equations (7-16) and (7-17), the probability function of the total pressure at time t, P(p), is given by

$$P(p) = P(k)\left|\frac{dk}{dp}\right|$$

$$= \frac{1}{\sqrt{2\pi}\beta t(2p_i - p)} \exp\left[-\frac{1}{2\beta^2 t^2} \ln^2 \left(\frac{2p_i - p}{2p_i - p_o}\right)\right] \qquad (7\text{-}19)$$

Therefore, the macroscopic (measured) total pressure at time t, $\bar{p}$, is given by

Table 7-1

The Thermal Decomposition of Azoisopropane

t (s)	p (torr)	$k \times 10^3$ (s^{-1})[161]
0	35.15	----
180	46.30	2.12
360	53.90	2.11
540	58.85	2.07
720	62.20	2.03
1020	65.55	1.96
		average 2.02

$$\bar{p} = \int_0^{2p_o} pP(p)\,dp \doteq \int_{-\infty}^{2p_o} pP(p)\,dp$$

$$= 2p_i - (2P_i - p_o)\exp\left(\frac{\beta^2 t^2}{2}\right) \qquad (7\text{-}20)$$

The calculated rate constant, k, is then given by

$$k = \frac{1}{t} \ln \frac{p_i}{2p_i - \bar{p}}$$

$$= k_o - \frac{\beta^2}{2} t \qquad (7\text{-}21)$$

The above equation shows that the calculated rate constant decreases with increasing time, as shown in Table 7-1. A least-square fitting of the above equation based on the data in Table 7-1 is shown in Figure 7-1. The time dependent rate constant is given by

$$k = 2.17 \times 10^{-3} - 1.99 \times 10^{-7}\, t \qquad (7\text{-}22)$$

Both the experimental result and the theory confirm that the calculated rate constant is not a constant, but a time dependent variable.

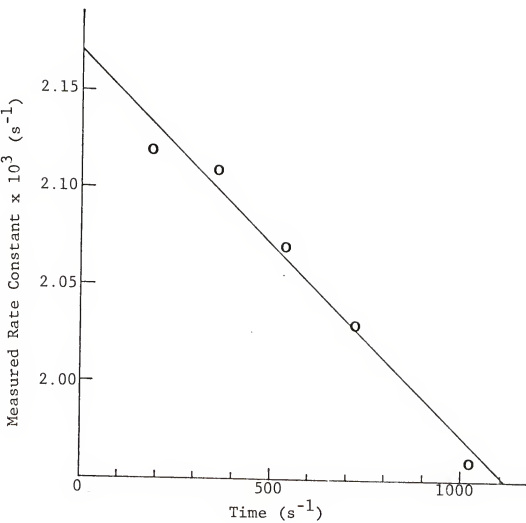

Fig. 7-1 - Time Dependence of the Rate Constant

CHAPTER VIII
GENERAL DISCUSSIONS ON THE LOGNORMAL DISTRIBUTION

Normal (Gaussian) Distribution

Suppose the variable z is distributed according to the normal distribution given by

$$P(z) = \frac{1}{\sqrt{2\pi}} \exp\left(-\frac{z^2}{2}\right), \text{ for } -\infty < z < \infty \qquad (8\text{-}1)$$

"It follows that the normal model (distribution) is strictly applicable only if· · ·negative measurements are possible."[18] "But many experimental variables are always positive (e.g., volume, mass, concentration, kinetic energy, absolute temperature, and the entropy change of an isolated system). In observations of variable of this sort, the Gaussian distribution function is often inappropriately applied - the experimental distribution is usually positively skewed."[16] The discussion for the distribution of the positive variables is given in the following section.

Two-Parameter Lognormal Distribution[162-167]

The two-parameter lognormal distribution, sometimes simply called lognormal distribution, is written as

$$P(x) = \begin{cases} \frac{1}{\sqrt{2\pi}\beta x} \exp\left(-\frac{1}{2\beta^2} \ln \frac{x}{x_o}\right), & \text{for } 0 \le x < \infty \\ 0, & \text{for } x \le 0 \end{cases} \tag{8-2}$$

where $x_o > 0$ and x_o is the geometrical mean of the variable x.[5] The above equation was obtained from Equation (8-1) through the transformation

$$z = \frac{1}{\beta} \ln \frac{x}{x_o} \tag{8-3}$$

In this distribution, one of the most important properties is that the standard deviation is proportional to the mean of the variable x as shown in Equation (2-39). It is interesting that many positive physical quantities can be described by this property. For example, the error in the weighing of a sample is usually assumed to be proportional to the weight in the analytical laboratory. In other words, the heavier the sample, the greater the error. In the quantitative analysis laboratory of the Department of Chemistry, the errors of students' reports are assumed to be proportional to the true values of their unknown samples. Therefore, the grading of students' reports of the unknown samples is based upon their relative errors. In analytical chemistry, the precision is usually expressed as the ratio of the standard deviation to the mean, i.e., the proportionality constant between the standard deviation and the mean, e.g., the relative error, or, as the ratio of the mean to the standard deviation, e.g., the signal-to-noise ratio or the spectral resolving power.

Another property in this distribution is that the logarithm

of a positive variable follows the normal distribution. Many positive physical quantities are expressed in the logarithmic forms, e.g., volume, pressure, concentration, activity coefficient in thermodynamics, wavelength, frequency and distance between electron and the nucleus.[162-166] The distribution of particle sizes is one of the best applications of the lognormal distribution. The distribution of particle sizes is usually given by

$$P(r) = \begin{cases} \frac{1}{\sqrt{2\pi}\beta_r r} \exp\left(-\frac{1}{2\beta_r^2} \ln^2 \frac{r}{r_o}\right), & \text{for } 0 \leq r < \infty \\ 0, & \text{for } r \leq 0 \end{cases} \quad (8\text{-}4)$$

where β_r is a dispersion parameter of the particle radius, r is the radius of the particle (m), and r_o is the geometrical mean of the radii (m), or the expected radius where $\beta_r = 0$.[33] The above equation was derived from Equation (8-1) through the transformation[5]

$$z = \frac{1}{\beta_r} \ln \frac{r}{r_o} \quad (8\text{-}5)$$

The lognormal distributions for the cross sections, Q (m^2), and the weights, W (kg), of particles can be derived from Equation (8-4) and written as

$$P(Q) = \frac{1}{\sqrt{2\pi}(2\beta_r)Q} \exp\left[-\frac{1}{2(2\beta_r)^2} \ln^2 \frac{Q}{Q_o}\right] \quad (8\text{-}6)$$

and

$$P(W) = \frac{1}{\sqrt{2\pi}(3\beta_r)W} \exp\left[-\frac{1}{2(3\beta_r)^2} \ln^2 \frac{W}{W_o}\right] \quad (8\text{-}7)$$

through the transformations

$$Q = \pi r^2 \tag{8-8}$$

$$Q_o = \pi r_o^2 \tag{8-9}$$

$$W = \frac{4}{3} \pi r^3 \rho \tag{8-10}$$

$$W_o = \frac{4}{3} \pi r_o^3 \rho \tag{8-11}$$

where ρ is the density of the particle (kg/m^3).

Define

$$\beta_Q = 2\beta_r \tag{8-12}$$

$$\beta_W = 3\beta_r \tag{8-13}$$

then

$$P(Q) = \frac{1}{\sqrt{2\pi}\beta_Q Q} \exp\left(-\frac{1}{2\beta_Q^2} \ln^2 \frac{Q}{Q_o}\right) \tag{8-14}$$

$$P(W) = \frac{1}{\sqrt{2\pi}\beta_W W} \exp\left(-\frac{1}{2\beta_W^2} \ln^2 \frac{W}{W_o}\right) \tag{8-15}$$

From Equations (8-4), (8-14) and (8-15), it is seen that if the particle radii follow the lognormal distribution, then the cross sections and the weights should also follow the lognormal distribution. However, it was shown that if the particle radii followed the normal distribution, then the cross sections or the weights would not follow the normal distribution.[5,21] From Equations (2-40) and (2-41), it is known that if the dispersion parameter is small, the normal distribution is an approximation of the lognormal distribution.[18] Because β_r is smaller than β_W, and if the normal

approximation is to be used, then the normal distribution gives a better approximation for the particle sizes than for particle weights. Yuan used the normal distribution for students' heights and the lognormal distribution for their weights in his theses.[5] This can be easily justified if it is assumed that the weight is roughly proportional to the third power of the height. From Equations (8-5), (8-6) and (8-7) one can find the following expressions given by

$$Q_{ave} \neq \pi r_{ave}^2$$

and

$$W_{ave} \neq \frac{4}{3} \pi r_{ave}^3 \rho$$

where r_{ave}, Q_{ave} and W_{ave} are the average radius, cross section and weight of the lognormally distributed particles. It is interesting to know that the above expressions do hold in the manipulation of data, as shown in the following example. Suppose there are two spherical particles with radii 1 and 3 (cm). Therefore, their cross sections are π and $q\pi$ (cm^2), respectively. The average radius and cross section are, respectively, given by

$$\begin{aligned} r_{ave} &= 2 \\ Q_{ave} &= 5\pi \end{aligned} \qquad (8\text{-}16)$$

It is seen from the above equations that $Q_{ave} \neq \pi r_{ave}^2$

The concentrations of many trace elements in geological samples were found to follow the lognormal distribution given by

$$P(C) = \frac{1}{\sqrt{2\pi}\beta C} \exp\left(-\frac{1}{2\beta^2} \ln^2 \frac{C}{C_o}\right) \quad (8\text{-}17)$$

where C is the concentration (M), and β is the dispersion parameter of the concentration.[73-77]

If the concentration of excited atoms follows the log-normal distribution, then the emission intensity in atomic emission spectroscopy, should follow the lognormal distribution. Equation (8-17) can be understood if it is assumed that the distribution of free energies of the samples follows the normal distribution. If it is assumed that the concentration of a material of interest (atom, ion or molecule) in an optical mdeium follows the lognormal distribution given by Equation (8-17), the distribution of the transmitted irradiances, P(I), through this medium, can be expressed as

$$P(I) = \frac{1}{\sqrt{2\pi}\beta I \ln (I_{oo}/I)} \exp\left[-\frac{1}{2\beta^2} \ln^2 \left(\frac{\ln I_{oo} - \ln I}{\ln I_{oo} - \ln I_o}\right)\right] \quad (8\text{-}18)$$

through the relations

$$\ln (I_{oo}/I) = \frac{1}{2.303} \varepsilon\, l\, C \quad (8\text{-}19)$$

$$\ln (I_{oo}/I_o) = \frac{1}{2.303} \varepsilon\, l\, C_o \quad (8\text{-}20)$$

where ε is the molar absorptivity ($M^{-1}cm^{-1}$) and l is the length of the optical medium (cm), I_{oo} is the incident irradiance and I_o is the transmitted irradiance when the medium is homogeneous.

If β in Equation (8-17) is very small, then Equation (8-17) becomes

$$P(C) = \frac{1}{\sqrt{2\pi}\beta C_o} \exp\left[-\frac{1}{2\beta^2 C_o^2}(C - C_o)^2\right] \qquad (8\text{-}21)$$

and the distribution of the transmitted irradiances follows the two-parameter lognormal distribution given by

$$P(I) = \frac{2.303}{\sqrt{2\pi}\varepsilon 1\beta C_o I} \exp\left(-\frac{2.303^2}{2\varepsilon^2 1^2 \beta^2 C_o^2} \ln^2 \frac{I}{I_o}\right) \qquad (8\text{-}22)$$

The above equation is identical with Equation (2-35) except for the notations for the dispersion parameter.

The lognormal distribution can also be applied to the study of the propagation of indeterminate error. In the case

$$R = AB/C \cdots\cdots \qquad (8\text{-}23)$$

one would inquire to "how scatter in measurements of quantities A, B, C etc., is translated into random variation in the final result R."[167] In the normal distribution, it is assumed that the errors are quadratically additive for independent processes. But in this case, the error of R is expressed as

$$\left(\frac{\sigma_R}{R}\right)^2 = \left(\frac{\sigma_A}{A}\right)^2 + \left(\frac{\sigma_B}{B}\right)^2 + \left(\frac{\sigma_C}{C}\right)^2 + \cdots \qquad (8\text{-}24)$$

where σ denotes the standard deviation, assuming that the standard deviations are approximately equal to the square roots of the variances.

It is interesting to note that in Equation (8-24), the assumption is that the relative errors, instead of the absolute errors, are quadratitally additive. If it is assumed that the lognormal distribution is applicable to Equation (8-23), i.e., the logarithms of the quantities follow the normal

distribution, then we have

$$\ln R = \ln A + \ln B + \ln C + \cdots \quad (8\text{-}25)$$

and

$$\sigma^2_{\ln R} = \sigma^2_{\ln A} + \sigma^2_{\ln B} + \sigma^2_{\ln C} + \cdots \quad (8\text{-}26)$$

assuming that the errors of the logarithms of the quantities are quadratically additive. If the errors are small, Equation (8-24) is found from Equation (8-26).

To evaluate the precision of an instrument, it is convenient to express the noise of a variable in terms of its logarithmic form. For example, let us evaluate the noise caused by a recorder. The signal, H, is assumed to be given by

$$H = R\,V \quad (8\text{-}27)$$

where H is the final output signal (cm), R is a conversion factor of the recorder (cm/V), and V is the output voltage of a detector (V).

The above equation gives

$$\sigma_H = (V\sigma_R)^2 + (R\sigma_V)^{2\,\frac{1}{2}} \quad (8\text{-}28)$$

If the noise from the recorder, N_R, is expressed as

$$N_R = V\sigma_R \quad (8\text{-}29)$$

and the overall noise from the detector, N_V, as

$$N_V = R\sigma_V \quad (8\text{-}30)$$

then the final output noise, σ_H, is given by

$$\sigma_H = (N_R^2 + N_V^2)^{\frac{1}{2}} \quad (8\text{-}31)$$

The above equation is used in the analytical laboratory,

assuming that N_R and N_V are independent. However, it is seen from Equations (8-29) and (8-30) that N_R and N_V are not independent at all. But, if we assume that the logarithms of the quantities in Equation (8-27) follow the normal distribution, so from Equation (8-27)

$$\ln H = \ln R + \ln V$$

then

$$\sigma^2_{\ln H} = \sigma^2_{\ln R} + \sigma^2_{\ln V} \tag{8-32}$$

then $\sigma_{\ln R}$ and $\sigma_{\ln V}$ are the independent noises. Hence, $\sigma_{\ln H}$ should be used to characterize the precision of the recorder function.

Three-Parameter Lognormal Distribution

Recently, a three-parameter lognormal distribution, P(I'), for the irradiance of an optical wave passing through the turbulent medium was proposed and experimentally verified.[123] The equation is given by

$$P(I') = \begin{cases} \dfrac{1}{\sqrt{2\pi}\beta(I' - I_1)} \exp\left[-\dfrac{1}{2\beta^2} \ln^2 \left(\dfrac{I' - I_1}{I_o}\right)\right], \\ \qquad\qquad\qquad\qquad \text{for } 0 \le I' \le \infty \\ 0, \qquad \text{for } I \le I_1 \end{cases} \tag{8-33}$$

where I' is the measured irradiances, I_1 and I_o are both positive constants, I_o is the geometrical mean of $(I - I_1)$,

and I_1 is called the lower limit of the transmitted irradiances. This distribution is also called the lognormal distribution with lower limit. It was derived empirically from Equation (8-1) through the transformation[5]

$$z = \frac{1}{\beta} \ln \left(\frac{I' - I_1}{I_o}\right) \tag{8-34}$$

Equation (8-33) can also be derived from Equation (2-35) by the relation

$$I' = I + I_1$$

where I' is the measured irradiance, I is the transmitted irradiance of the light beam from the source, and I_1 is the background irradiance which is a constant.

In a gas chromatograph, the retention time of a sample, t, should have a lower limit, t_a, which is the retention time of the air peak. Thus, the shape of a sample peak in the gas chromatograph might be reasonably expressed as

$$P(t) = \frac{1}{\sqrt{2\pi}\beta(t - t_a)} \exp\left[-\frac{1}{2\beta^2} \ln^2 \left(\frac{t - t_a}{t_o}\right)\right] \tag{8-35}$$

where t_o is the geometrical mean of $(t - t_a)$ and β is a dispersion parameter of the sample for the broadening of a peak. The above equation is plotted in Figure 8-1. The curves in Figure 8-1, generated from a simple empirical equation, are similar to those shown in Figure 8-2 proposed by Li.[168] A theoretical curve based on the binomial (Bernoulli's) distribution is duplicated in Figure 8-3, for comparison, showing that the shape of a sample peak is skewed and has a lower limit.[169] It is seen that the three-parameter model is good and convenient.

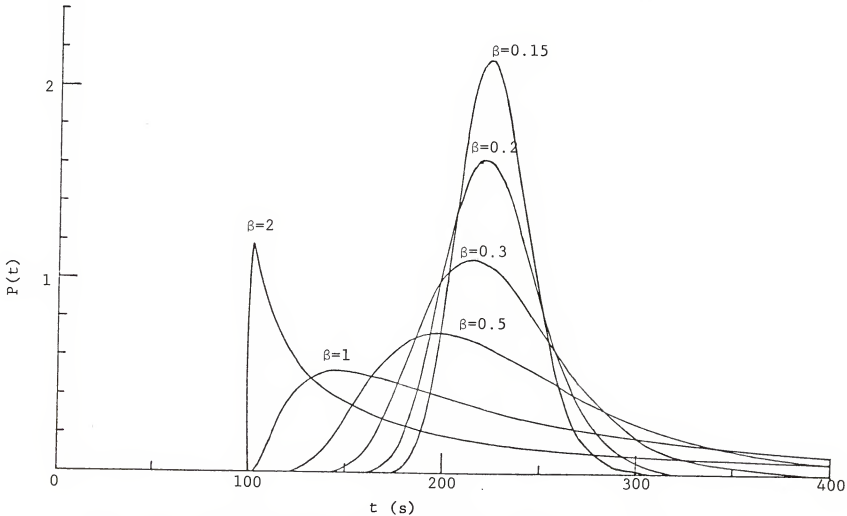

Fig. 8-1 - Shape of the Gas Chromatographic Peaks (t_a = 100; t_o = 126)

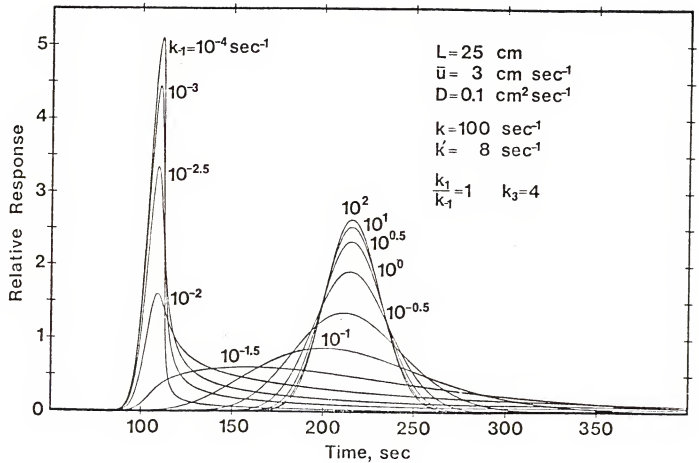

Fig. 8-2 - Shape of the Gas Chromatographic Peaks

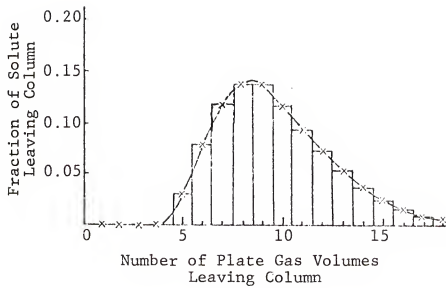

Fig. 8-3 - Elution Curve for One Unit of Solute From Five-Plate Column

The time, t_{max}, where the peak is maximum in Equation (8-35), is given by

$$t_{max} = t_a + t_o \exp(-\beta^2) \tag{8-36}$$

and the maximum peak height, h, is therefore

$$h = \frac{1}{\sqrt{2\pi}\beta t_o} \exp\left(\frac{\beta^2}{2}\right) \tag{8-37}$$

The area under the curve, A, is unity. Using the expression for the number of theoretical plates, N, given by

$$N = 2\pi \left(\frac{h t_{max}}{A}\right)^2 \tag{8-38}$$

and from Equations (8-36), (8-37) and (8-38), the number of theoretical plates is given by[169]

$$N = \frac{1}{\beta^2 t_o^2} \exp(\beta^2) \; t_a + t_o \exp(-\beta^2) \tag{8-39}$$

The above equation is plotted in Figure 8-4. It is shown in Figure 8-4 that the number of theoretical plates decreases then increases with increasing β.

Four-Parameter Lognormal Distribution

The four-parameter lognormal distribution is an extension of the normal distribution to allow for both a lower and upper limit to the possible values of the variable, given by

$$P(x) = \frac{1}{\sqrt{2\pi}\beta} \left(\frac{1}{x_u - x} + \frac{1}{x - x_1}\right) x$$

$$\exp\left[-\frac{1}{2\beta^2} \left(\ln \frac{x - x_1}{x_u - x} - \ln \frac{x_o - x_1}{x_u - x_o}\right)\right],$$

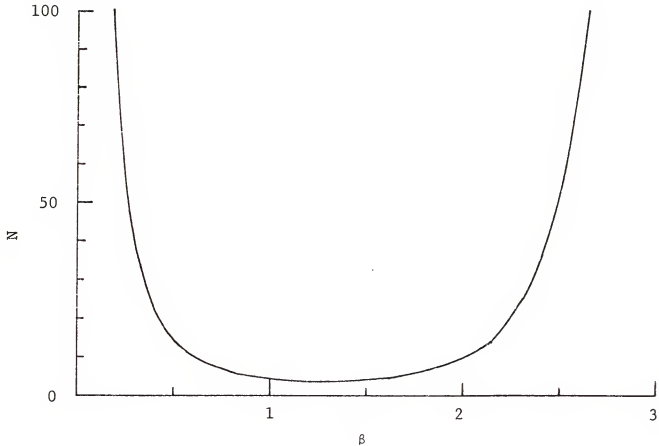

Fig. 8-4 - Number of Theoretical Plates.

$$P(x) = \begin{cases} \text{for } x_l \le x \le x_u \\ 0, \quad \text{for } x \le x_l \quad \text{or} \quad x \le x_u \end{cases} \tag{8-40}$$

where x_u and x_l is the upper and the lower limit of the variable x, and $(x_o - x_l)/(x_u - x_o)$ is the geometrical mean of $(x - x_l)/(x_u - x)$.

The above equation was derived from Equation (8-1) through the transformation

$$z = \frac{1}{2\beta} \left(\ln \frac{x - x_l}{x_u - x} - \ln \frac{x_o - x_l}{x_u - x_o} \right) \tag{8-41}$$

Equation (8-40) was used to study the distribution of the percentages of the lawns covered by clover, by letting x denote the percentage of coverage, $x_o = 0$, and $x_u = 100$.[11] It was used to study the distribution of the droplet sizes with an upper limit of droplet size, by letting x denote the diameter of the particle and $x_l = 0$. The above empirical approach was experimentally shown to be better than the empirical Rosin-Rawmler equation, and the semi-empirical Nukiyama-Tanaswa equation.[170,171]

Folded Lognormal Distribution

This distribution was derived from the model of random walk with reflecting barrier for the distribution of the droplet size with an upper limit, given by

$$P(x) = \begin{cases} \dfrac{1}{\sqrt{2\pi}\beta x} \exp\left(-\dfrac{1}{2\beta^2} \ln \dfrac{x}{x_o}\right) \\ \quad + \dfrac{1}{\sqrt{2\pi}\beta x} \exp\left[-\dfrac{(2 \ln x_m - \ln x x_o)^2}{2^2}\right], \\ \qquad\qquad \text{for } 0 \le x \le x_m \\ 0, \qquad\qquad \text{for } 0 \le x \end{cases} \tag{8-42}$$

where x is the droplet diameter (m) and x_u is the maximum diameter (m).[36,132]

If the droplet size decreases due to the evaporation, the droplet diameter at any time, x_t, is given by

$$x_t^2 = x^2 - kt \tag{8-43}$$

where k ($m^2\ s^{-1}$) is an evaporation constant.[172]

The distribution of the droplet sizes at any time will be given by

$$P(x_t) = \begin{cases} \dfrac{x_t}{\sqrt{2\pi}\beta(x_t^2 + kt)} \exp\left[-\dfrac{1}{8\beta^2} \ln^2 \left(\dfrac{x_t^2 + kt}{x_{o,t}^2 + kt}\right)\right] \\ \quad + \dfrac{x_t}{\sqrt{2\pi}\beta(x_t^2 + kt)} \exp\left\{-\dfrac{1}{8^2}\left[2 \ln (x_{m,t}^2 + kt)\right.\right. \\ \quad + \left.\left. \ln (x_t^2 + kt)(x_{o,t}^2 + kt)\right]\right\}, \\ \qquad\qquad \text{for } 0 \le x \le (x_m^2 - kt)^{\frac{1}{2}} \\ 0, \qquad \text{for } x_t \le 0 \quad \text{or} \quad x_t \ge (x_m^2 - kt)^{\frac{1}{2}} \end{cases} \tag{8-44}$$

where the maximum diameter $x_{m,t}$ and the geometrical mean of

diameters, $x_{o,t}$ at any time are given by, respectively

$$x_{m,t}^2 = x_m^2 - kt$$

$$x_{o,t}^2 = x_o^2 - kt$$

Equation (8-44) can be used for the time dependent distribution of droplet sizes in the atomic flame spectroscopy.

Relationships among the Lognormal Distributions

A three-parameter lognormal distribution, as in Equations (8-33) or (8-35), can be reduced to a two-parameter lognormal distribution, as in Equation (8-4), if the lower limit is zero, i.e., $I_u = 0$ or $t_a = 0$. A four-parameter lognormal distribution, such as in Equation (8-40), can be reduced to a three-parameter lognormal distribution, as in Equation (8-33) or (8-34), if the upper limit is infinite and it can further be reduced to a two-parameter distribution if the upper limit is infinite and the lower limit is zero. Similarly, a folded lognormal distribution, such as in Equation (8-42), can be reduced to a two-parameter lognormal distribution if the upper limit is infinite.

CHAPTER IX
INTERFERENCE ON MAGNESIUM BY TRACE CONCOMITANTS IN FLAME ATOMIC ABSORPTION SPECTROMETRY

Concomitant interferences remain one of the major sources of inaccuracy in flame atomic absorption spectrometry. Most previous efforts emphasize interferences due to large excesses of concomitants in the sample matrices. In this chapter, the interferences by the presence of trace concomitants (on magnesium), which have been generally ignored in flame atomic absorption spectrometry are reported.

Experimental

Observations were made with Perkin-Elmer Model 303 atomic absorption spectrometer (Perkin-Elmer, Norwalk, Conn.) with a 10 cm burner for an air/acetylene flame. A Ca-Mg-Al hollow cathode lamp (Varian Techtron, Palo Alto, Calif.) was used in all studies; the image of the light source was 3 mm in diameter on the focal plane; the monochromator was adjusted to 2852 Å for magnesium with 1 mm slit width. A magnesium stock solution was prepared directly by dissolving reagent grade magnesium sulfate; an aluminum stock solution was prepared from reagent grade aluminum chloride and gravimetrically determined. Serial dilutions were carried

with deionized water. In several studies, an electric field at 50 V cm^{-1} was applied across the sprayer and the burner head of the nebulizer-burner.

Results and Discussion

Analytical Growth Curves

The analytical curves for magnesium are depicted in Figure 9-1 for several flame heights and for acetylene and air flow rates of 4.3 and 28.7 l min^{-1}, respectively. The slopes of the analytical curves at 1.5 mm, 2.5 mm and 5 mm are less than unity. In the low region (1.5 - 5.0 mm) of the flame, magnesium does not have enough time travelling upward in the flame to receive sufficient thermal-collisional energy to atomize. The slow rate of volatization is most likely responsible for the departure of the slopes from unity. According to the Nukiyama-Tanasawa expression, the concentration of $MgSO_4$ in solution does not affect the size of sprayed droplets in the nebulizing chamber.[171] The lowering of the vapor pressure of the droplet due to the presence of salt in the droplet can be qualitatively understood by

$$\frac{P_r}{P_\infty} = \{\exp\left(\frac{2\sigma M}{\rho RTr}\right)\}\{1 - \frac{4\pi m M}{3\pi r^3 \rho W}\} \qquad (9\text{-}1)$$

where P_r is the equilibrium vapor pressure of water over a droplet of radius r (cm) and density ρ (g cm^{-3}) containing m (g) of the dissolved $MgSO_4$, P_∞ is the equilibrium vapor pressure over a flat surface of water at the same temperature

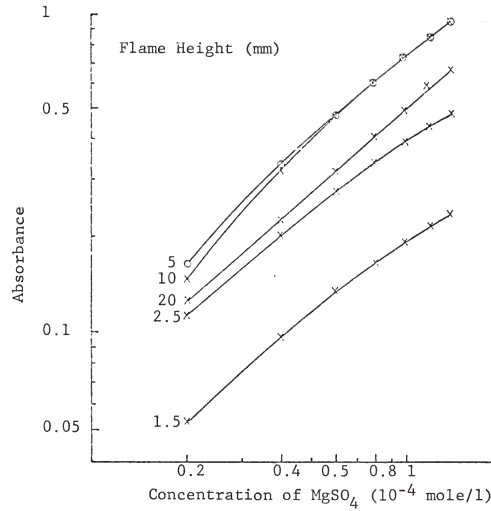

Fig. 9-1 - Analytical Curves of Magnesium

T (°K), (dyne cm^{-2}) is the surface tension of water at temperature T, I is van't Hoff's factor, W and M are the molecular weights of $MgSO_4$ and water, respectively, and R is the gas constant.[173] From the above thermodynamic equation, it can be seen that the vapor pressure of water over the droplet can be reduced significantly by the presence of dissolved salt, if the size of the droplet is extremely small. Therefore, the rate of desolvation would be expected to be significantly reduced by the presence of salt in the droplet, when the droplet does not have enough time to evaporate the solvent in the low, cool region of the flame. After the desolvation is completed, the size of dried magnesium particulate will depend upon the original solution concentration. After desolvation, the resulting particulate melts. Large particulates should result in a lesser lowering of the melting point than small particulates according to the Thomson equation

$$\frac{\Delta T_m}{T_m} = \frac{2\sigma V}{Lr} \qquad (9\text{-}2)$$

where T_m is the lowering of melting point of a spherical solid particulate relative to the macroscopic melting point T_m, σ (dyne cm^{-1}) and V (cm^3 $mole^{-1}$) are the surface tension and molar volume of the dried particulate at the melting point, respectively, and L (erg $mole^{-1}$) is the heat of melting.[174]

The decrease in vapor pressure of a large molten droplet is expressed by the Kelvin equation

$$\frac{P_r}{P_\infty} = \exp\left(\frac{2\sigma M}{\rho RTr}\right) \qquad (9\text{-}3)$$

where the physical parameters are those of the molten droplet.[175] Also, a large molten droplet results in slow vaporization because of the small surface/mass ratio. All of the successive factors, low vapor pressure of solution (water) droplets, high melting point of solid particulates, low vapor pressure and low surface/mass ratio of molten droplets for a droplet formed initially from a solution of high concentration, are present and cause the reduction in the slope of the analytical curve of magnesium in the low, cool region of the flame. The slope of the analytical curve at a 10 mm measurement height (above burner top) is about unity. The slope of the analytical curve at a 20 mm height is less than unity but larger than those at 1.5 mm and 2.5 mm measurement heights.

At a measurement height of 20 mm, magnesium salt particles have more time travelling upward in the flame to allow for the processes of solvent evaporation and solute vaporization. The rate of volatization of magnesium salts would appear to be relatively unimportant. The negative deviation of the analytical curve from a slope of one is probably a result of the lognormal distribution of the transmitted intensities due to the turbulence of the flame at 20 mm. If it is assumed that the transmitted intensities of a beam of radiation can be described by Equation (8-22), then the average transmitted intensity measured, I_{ave}, is given by

$$I_{ave} = \int_0^{\infty} I\, P(I)\, dI$$

$$= I_o \exp\left[\frac{1}{2}\left(\frac{\varepsilon l \beta C_o}{2.303}\right)^2\right]$$

where I_o is the transmitted intensity when there is no turbulence of the concentration of magnesium atoms in the optical region of the flame, ε is the molar absorptivity (M^{-1} cm^{-1}) of magnesium atoms, l (cm) is the horizontal length of the flame at 20 mm, β is a dimensionless parameter for the dispersion of transmitted intensities and C_o (M) is the concentration of magnesium atoms when the flame is homogeneous.

From the above equation, the average (measured) absorbance of the inhomogeneous region of the flame is given by

$$A_{in} = \log\left(\frac{I_{oo}}{I_{ave}}\right)$$

$$= \varepsilon\, l\, C_o\, (1 - 1.152\, \beta\, \varepsilon\, l\, C_o)$$

where I_{oo} is the incident intensity.

It is seen in the above equation that the measured absorbance will show a negative deviation, due to the turbulence of the flame, as C_o increases.

Interferences

Interferences of magnesium in solutions of 10^{-4} M $MgSO_4$ and various concentrations of $AlCl_3$ are shown in Figure 9-2. Flow rates are the same as those used for the data in Figure 9-1. The interference curve of Mg by $AlCl_3$ is generally flat at a 20 mm height above the burner top. The matrix effect is visible at high concentrations of $AlCl_3$. It is reasonable

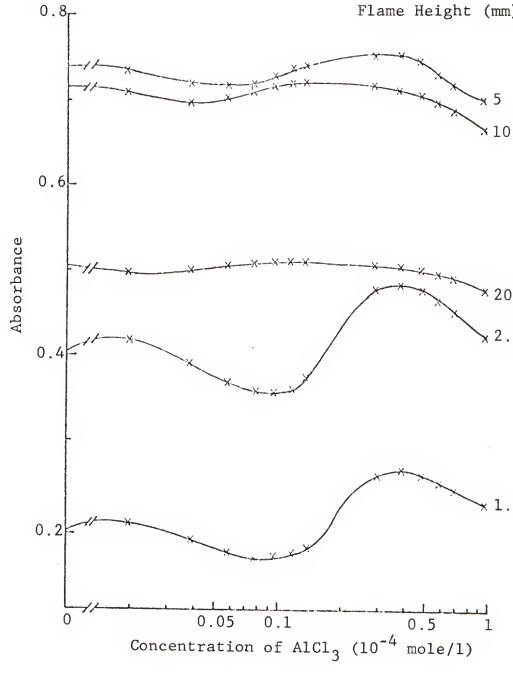

Fig. 9-2 - Interference Curves of Magnesium by Aluminum Chloride

to conclude from the curve at 20 mm that the presence of $AlCl_3$ for the range of Mg concentrations studied does not affect the size of droplets sprayed and the nebulization efficienty of the solutions.[171] The interference curves at 1.5 mm and 2.5 mm look peculiar but are in good agreement with that obtained by Menzies.[176] However, the present curves are more detailed in the low concentration range of $AlCl_3$. It seems obvious that the peculiar shapes of interference curves in the lower region of the flame is due to the presence of some unknown eutectic mixtures of magnesium-aluminum compounds and the mass-controlled processes of vaporization. Measurements at 5 mm and 10 mm heights result in higher signals than at 20 mm but suffer more interferences. Practically, it would be advisable to gain accuracy at the sacrifice of signal intensity by looking at higher parts of the flame.

The data in Figure 9-3 were obtained by changing the flow rate of acetylene and by applying the electric field across the sprayer and burner head. The flow rate of air was the same as mentioned above. Higher flow rates of acetylene enhanced the signal at a 20 mm height but reduced the signal at a 2.5 mm height when no electric field was applied. Higher flow rates of acetylene caused the transit time of magnesium to be shorter. Therefore, signals are lower and interferences are greater at lower heights with higher fuel flow rates. Also, higher flow rates of acetylene would result in a larger, more reducing flame and so the absorption

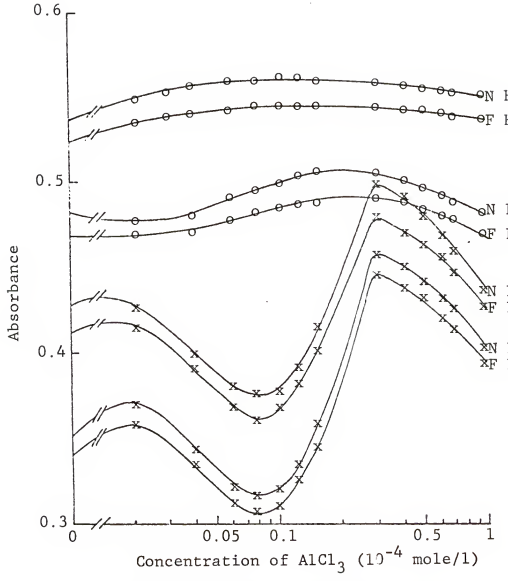

Fig. 9-3 - Effects of Acetylene Flow Rate, Flame Height and Electric Field on the Interference Curves H: Acetylene, 5l/min.; L: Acetylene, 4.3 l/min.; -o-: 20 mm above Burner Head; -x-: 2.5 mm above Burner Head; N: Normal Operation; F: With Applied Electric Field.

signals are larger and interferences are less in higher parts of the flame. To reduce the interference, the slightly fuel-rich flame is favorable with measurements in the higher parts of the flame. The parallelism between the interference curves with and without electric field indicates that the decreased signals when the electric field was applied might be due to the increased rates of coalescence and/or deposition of the sprayed droplets on the walls and spoiler of the nebulizing chamber by means of electrostatic effects.[177]

The interference curves of magnesium by $AlCl_3$ in the presence of 0.1 M HCl were generally flat and slightly bent down at high concentration of $AlCl_3$. To reduce chemical interferences due to trace concentration of $AlCl_3$. HCl should be added to the measured solutions.

PART II

DETERMINATE ERRORS IN UV-VISIBLE MOLECULAR ABSORPTION SPECTROSCOPY

CHAPTER X
DETERMINATE ERRORS IN ULTRAVIOLET AND VISIBLE SPECTROPHOTOMETRIC MEASUREMENTS CAUSED BY MULTIPLE REFLECTIONS WITHIN THE CELL

Absorption spectrophotometry has been a widely used analytical tool. Departures from Beer's law due to multiple reflections within the cell have been quantitatively approximated in the past by other workers.[178-182] The departures were expressed in terms of absorbance errors and correction factors for the measured fraction of light absorbed.[178-182] Positive deviation of absorbance should result in a correction factor of less than unity for the measured fraction of light absorbed. However, contradictions arise when attempting to correlate the positive absorbance errors and correction factors of greater than unity.[178-182] To remove the confusion and to allow a better understanding of the factors leading to greater accuracy in absorption spectrophotometry, a more rigorous approach to the effects caused by multiple reflections within the cell is required.

Theoretical Considerations

When radiation passes through an interface between two transparent semi-infinite media of different refractive indi-

ces, a fraction of the radiation is reflected at the interface. If the incident angle is zero, as is normally the case in absorption spectrophotometry, the fraction of light reflected is

$$f = \frac{n_1 - n_2}{n_1 + n_2} \tag{10-1}$$

where n_1 and n_2 are the refractive indices of the two media comprising the interface. When a parallel beam of monochromatic radiation with zero incident angle passes from one transparent semi-infinite medium to another transparent semi-infinite medium through a window of internal transmittance, t_w, the actual fractions fo the light transmitted, reflected and absorbed due to multiple reflections of the radiation within the parallel surfaces of the window are t_{12}, r_{12} and α_{12}, respectively. In Figure 10-1 the fractions transmitted, reflected and absorbed are shown. By considering the processes of transmission, reflection and absorption at the two interfaces, the fractions transmitted, t_{12}, reflected, r_{12}, and absorbed, α_{12}, are given by

$$t_{12} = (1 - f_1)(1 - f_2)t_w(1 + f_1 f_2 t_w^2 + \cdots) \tag{10-2a}$$

$$t_{12} = \frac{(1 - f_1)(1 - f_2)t_w}{1 - f_1 f_2 t_w^2} \tag{10-2b}$$

$$r_{12} = f_1 + (1 - f_1)^2 f_2 t_w^2(1 + f_1 f_2 t_w^2 + \cdots) \tag{10-3a}$$

$$r_{12} = \frac{f_1 - 2f_1 f_2 t_w^2 + f_2 t_w^2}{1 - f_1 f_2 t_w^2} \tag{10-3b}$$

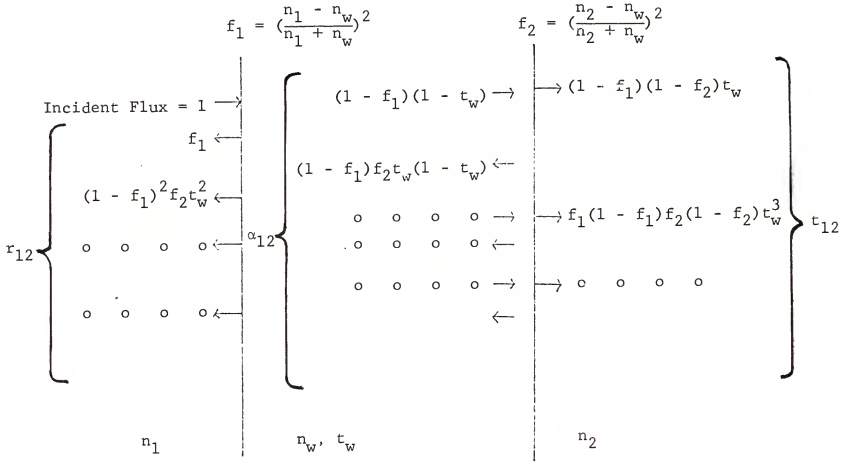

Fig. 10-1 - Actual Fractions of Radiation Transmitted, t_{12}, Reflected, r_{12}, and Absorbed, α_{12}, when Radiation Passes from Medium 1 to Medium 2 Perpendicularly through a Window. It is Assumed that the Initial Flux Incident on the Front Window is Unity.

$$\alpha_{12} = (1 - f_1)(1 - t_w)(1 + f_1 f_2 t_w^2 + \cdots) \qquad (10\text{-}4a)$$

$$\alpha_{12} = \frac{(1 - f_1)(1 + f_2 t_w)(1 - t_w)}{1 - f_1 f_2 t_w^2} \qquad (10\text{-}4b)$$

Similarly, when the radiation passes in the opposite direction from medium 2 to medium 1 through the same window with zero incident angle, the fractions of radiation transmitted, t_{21}, reflected, r_{21}, and absorbed, α_{21}, are also given by

$$t_{21} = \frac{(1 - f_1)(1 - f_2)t_w}{1 - f_1 f_2 t_w^2} \qquad (10\text{-}2b)$$

$$r_{12} = \frac{f_1 f_2^2 - 2f_1 f_2 t_w^2 + f_2}{1 - f_1 f_2 t_w^2} \qquad (10\text{-}5)$$

$$\alpha_{12} = \frac{(1 + f_1 t_w)(1 - f_2)(1 - t_w)}{1 - f_1 f_2 t_w^2} \qquad (10\text{-}6)$$

The above equations show that only transmittance is symmetric with respect to the direction of light.

In order to develop realistic expressions for absorption spectrophotometry consider an absorption cell consisting of two identical parallel windows separated by a parallel column of absorbing medium (the sample which is assumed to be homogeneous) of transmittance, t_s. When a parallel beam of monochromatic radiation passes through the cell with zero incident angles, the fractions of light transmitted, T_t, reflected, R_t, and absorbed, α_t, due to multiple reflections within the cell (see Figure 10-2) are given by

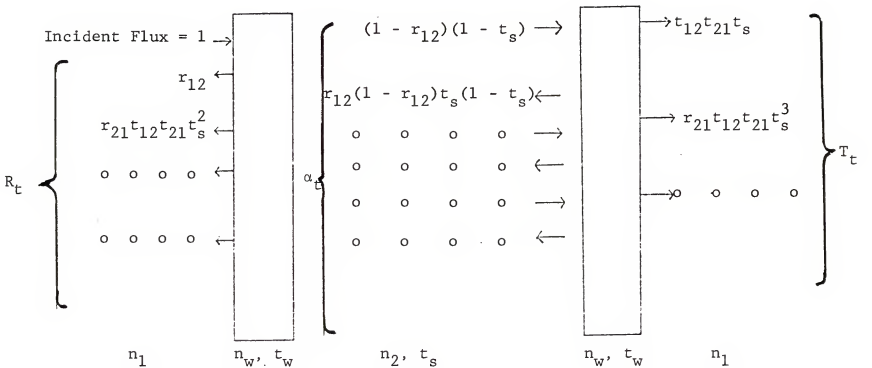

Fig. 10-2 - Actual Fractions of Radiation Transmitted, T_t, Reflected, R_t, and Absorbed, α_t, when Radiation Passes Perpendicularly through a Cell. It is Assumed that the Initial Flux Incident upon the Front Window of the Cell is Unity.

$$T_t = t_{12}t_{21}t_s(1 + r_{21}^2 t_s + \cdots) \qquad (10\text{-}7a)$$

$$T_t = \frac{t_{12}t_{21}t_s}{1 - r_{21}^2 t_s^2} \qquad (10\text{-}7b)$$

$$R_t = r_{12} + r_{21}t_{12}t_{21}t_s^2(1 + r_{21}^2 t_s^2 + \cdots) \qquad (10\text{-}8a)$$

$$R_t = r_{12} + \frac{r_{21}t_{12}t_{21}t_s^2}{1 - r_{21}^2 t_s^2} \qquad (10\text{-}8b)$$

$$\alpha_t = (1 - r_{12})(1 - t_s)(1 + r_{21}^2 t_s + \cdots) + (1 - r_{12})(1 - t_s)r_{21}t_s(1 + r_{21}^2 t_s + \cdots) \qquad (10\text{-}9a)$$

$$\alpha_t = \frac{(1 - r_{12})(1 - t_s)}{1 - r_{21}t_s} \qquad (10\text{-}9b)$$

To simplify the derivations, the following assumptions are made:

(i) the radiation is monochromatic;[183]

(ii) the cell windows are flat, have parallel sides, and have no imperfections;

(iii) the optical alignment allows only zero incident angles at the interfaces of interest;

(iv) the temperature, pressure and reflactive index are the same in the light path and in the surrounding of the path; thermo-optic effects are absent;

(v) The absorber is isotropic, non-fluorescent, non-black-body radiative and homogeneous; the absorber results in no Bragg diffraction, no dichroism and

no Mie scattering; i.e., there are no solid or liquid crystals formed, and all particles are much smaller than the wavelengths of interest in the absorber;[184]

(vi) the Fabry-Perot interferometric line spacings are too small to be resolved by the detector;[184]

(vii) Beer's law is valid at all concentrations; there are no association, dissociation, and cross-interaction processes which cause deviations; the absorptivity coefficient is also constant;

(viii) when two cells are in use, they are identical;

(ix) the radiation is low enough to guarantee no saturation of excited levels of the absorbing solute and there are no other systematic errors;[185]

(x) finally, window absorption of commercial fused silica, solvent absorption, band overlapping of various components at the wavelength of interest, and the variation of refractive index of the solution at low concentrations are all assumed absent.[186,187]

Therefore, Equations (10-1) through (10-6) can be reduced to

$$t = \frac{(1 - f_1)(1 - f_2)}{1 - f_1 f_2} ; \quad (t = t_{12} = t_{21}) \qquad (10\text{-}10)$$

$$r = \frac{f_1 - 2f_1 f_2 + f_2}{1 - f_1 f_2} ; \quad (r = r_{12} = r_{21}) \qquad (10\text{-}11)$$

where t is the fraction transmitted for one of the cell windows ($t_w = 1$), r is the fraction reflected for one of the cell

windows ($t_w = 1$), and $\alpha = 0$ since $t_w = 1$ according to the above assumptions, and therefore Equations (10-7) through (10-9) for the fractions of radiation transmitted, T_t, reflected, R_t, and absorbed, α_t, when radiation passes through the cell can be reduced to

$$T_t = \frac{t^2 t_s}{1 - r^2 t_s^2} \tag{10-12}$$

$$R_t = r + \frac{r t^2 t_s^2}{1 - r^2 t_s^2} \tag{10-13}$$

$$\alpha_t = \frac{(1 - r)(1 - t_s)}{1 - r t_s} \tag{10-14}$$

Absorbance Error and Correction Factors

The relative absorbance error is defined as

$$\delta A = \frac{A_{meas} - A_{sol}}{A_{sol}} \tag{10-15}$$

where A_{sol} is the true solution absorbance and A_{meas} is the apparent (measured) absorbance. Because $t_s = 1$ for the reference cell filled with pure solvent, the apparent (measured) transmittance of the solution is given by

$$t_{meas} = \frac{(T_t)_{sol}}{(T_t)_{solv}}$$

$$t_{meas} = \frac{(1 - r^2) t_s}{1 - r^2 t_s^2} \tag{10-16}$$

where $(t_t)_{sol}$ is the fraction of radiation transmitted through

the sample cell containing sample solution and $(T_t)_{solv}$ is the fraction of radiation transmitted through the same cell containing solvent. Hence, the apparent (measured) absorbance is given by

$$A_{meas} = A_{sol} + \log \left(\frac{1 - r^2 t_s^2}{1 - r^2}\right) \qquad (10\text{-}17)$$

Equation (10-15) can be rewritten as

$$\delta A = \frac{\log\left(\frac{1 - r^2}{1 - r^2 t_s^2}\right)}{\log (t_s)} \qquad (10\text{-}18)$$

The calculations of the relative absorbance error at 25°C were carried out and tabulated in Table 10-1 for aqueous and air solutions assuming Corning 7940 fused silica windows.[188,189]

Correction Factor for Actual Fraction of Radiation Absorbed

An expression which gives correction factors for the actual fraction of light absorbed by the sample is

$$F_{act} = \frac{\alpha_t}{\alpha_{meas}} = \frac{\alpha_t}{1 - t_{meas}} \qquad (10\text{-}19)$$

i.e.,

$$F_{act} = \frac{(1 - r)(1 + r t_s)}{1 + r^2 t_s} \qquad (10\text{-}20)$$

where the measured fraction of light absorbed, α_{meas}, is defined as

$$\alpha_{meas} = 1 - t_{meas} \qquad (10\text{-}21)$$

Table 10-1

Relative Absorbance Error (Parts per Thousand)
Due to Multiple Reflections

	Wavelength (nm)					
	275		468		656	
Absorbance	Aqueous	Air	Aqueous	Air	Aqueous	Air
0.00	3.43	11.62	2.80	9.45	2.66	8.95
0.05	3.07	10.37	2.50	8.44	2.37	7.99
0.10	2.75	9.30	2.24	7.57	2.13	7.17
0.15	2.48	8.38	2.02	6.82	1.92	6.46
0.20	2.24	7.58	1.83	6.17	1.73	5.84
0.25	2.04	6.89	1.66	5.60	1.58	5.31
0.30	1.86	6.29	1.52	5.11	1.44	4.84
0.35	1.70	5.76	1.39	4.68	1.32	4.44
0.40	1.57	5.30	1.28	4.31	1.21	4.08
0.45	1.45	4.89	1.18	3.98	1.12	3.77
0.50	1.34	4.53	1.09	3.69	1.04	3.49
0.55	1.25	4.21	1.02	3.43	0.96	3.25
0.60	1.16	3.93	0.95	3.20	0.90	3.03
0.65	1.09	3.68	0.89	2.99	0.84	2.83
0.70	1.02	3.45	0.83	2.81	0.79	2.66
0.75	0.96	3.25	0.79	2.64	0.74	2.50
0.80	0.91	3.07	0.74	2.50	0.70	2.36
0.85	0.86	2.90	0.70	2.36	0.66	2.24
0.90	0.82	2.75	0.67	2.24	0.63	2.12
0.95	0.77	2.62	0.63	2.13	0.60	2.02
1.00	0.74	2.49	0.60	2.03	0.57	1.92
1.05	0.70	2.38	0.57	1.93	0.54	1.83
1.10	0.67	2.27	0.55	1.85	0.52	1.75
1.15	0.65	2.18	0.53	1.77	0.50	1.68
1.20	0.62	2.09	0.50	1.70	0.48	1.61
1.25	0.59	2.01	0.49	1.63	0.46	1.55
1.30	0.57	1.93	0.47	1.57	0.44	1.49
1.35	0.55	1.86	0.45	1.51	0.43	1.43
1.40	0.53	1.80	0.43	1.46	0.41	1.38
1.45	0.51	1.73	0.42	1.41	0.40	1.34
1.50	0.50	1.68	0.41	1.36	0.38	1.29
1.55	0.48	1.62	0.39	1.32	0.37	1.25
1.60	0.47	1.57	0.38	1.28	0.36	1.21
1.65	0.45	1.52	0.37	1.24	0.35	1.18
1.70	0.44	1.48	0.36	1.20	0.34	1.14
1.75	0.43	1.44	0.35	1.17	0.33	1.11
1.80	0.41	1.40	0.34	1.14	0.32	1.08
1.85	0.40	1.36	0.33	1.11	0.31	1.05
1.90	0.39	1.32	0.32	1.08	0.30	1.02
1.95	0.38	1.29	0.31	1.05	0.30	0.99
2.00	0.37	1.26	0.30	1.02	0.29	0.97

Rewriting Equation (10-16), we have

$$t_s = \frac{r^2 - 1 + \sqrt{[(1 - r^2)^2 + 4r^2 t_{meas}^2}}{2r^2 t_{meas}} \qquad (10\text{-}22)$$

The calculations of the correction factor for actual fraction of light absorbed at 25°C were carried out and tabulated in Table 10-2 for aqueous and air solutions for fused silica windows.[188-190]

Correction Factor for Theoretical Fraction of Radiation Absorbed

Correction factors for theoretical fraction of light absorbed by the sample without multiple reflections are defined as

$$F_{theo} = \frac{1 - t_s}{\alpha_{meas}} = \frac{1 - t_s}{1 - t_{meas}} \qquad (10\text{-}23)$$

and by use of the previous expressions is found to be

$$F_{theo} = \frac{1 - r^2 t_s^2}{1 + r^2 t_s^2} \qquad (10\text{-}24)$$

The calculations of correction factors for the theoretical fraction of light absorbed at 25°C were carried out and tabulated in Table 10-3 for aqueous and air solutions for fused silica windows.[188,189]

Relative Increase of Sensitivity of Absorbance Due to Multiple Reflections

The relative increase of sensitivity of absorbance due to

Table 10-2

Correction Factors for Actual Fraction of Light Absorbed

Measured Fraction of Light Absorbed	Wavelength (nm)					
	275		468		656	
	Aqueous	Air	Aqueous	Air	Aqueous	Air
0.0	0.9966	0.9885	0.9972	0.9906	0.9974	0.9911
0.1	0.9928	0.9822	0.9938	0.9848	0.9940	0.9854
0.2	0.9890	0.9758	0.9903	0.9789	0.9906	0.9797
0.3	0.9852	0.9694	0.9869	0.9730	0.9873	0.9739
0.4	0.9814	0.9629	0.9833	0.9671	0.9839	0.9681
0.5	0.9776	0.9565	0.9799	0.9612	0.9805	0.9624
0.6	0.9738	0.9500	0.9765	0.9553	0.9771	0.9566
0.7	0.9700	0.9435	0.9730	0.9493	0.9737	0.9507
0.8	0.9662	0.9370	0.9695	0.9434	0.9704	0.9449
0.9	0.9624	0.9305	0.9661	0.9374	0.9670	0.9391

Table 10-3

Correction Factors for Theoretical Fraction of Light Absorbed

Measured Fraction of Light Absorbed	Wavelength (nm)					
	275		468		656	
	Aqueous	Air	Aqueous	Air	Aqueous	Air
0.0	0.9966	0.9885	0.9972	0.9906	0.9974	0.9911
0.1	0.9971	0.9902	0.9976	0.9920	0.9977	0.9924
0.2	0.9975	0.9917	0.9980	0.9932	0.9981	0.9936
0.3	0.9980	0.9931	0.9983	0.9914	0.9984	0.9947
0.4	0.9984	0.9945	0.9987	0.9955	0.9987	0.9957
0.5	0.9987	0.9957	0.9990	0.9965	0.9990	0.9967
0.6	0.9990	0.9968	0.9992	0.9974	0.9993	0.9975
0.7	0.9993	0.9977	0.9995	0.9982	0.9995	0.9983
0.8	0.9996	0.9986	0.9997	0.9989	0.9997	0.9989
0.9	0.9998	0.9994	0.9999	0.9995	0.9990	0.9995

multiple reflections within the cell is defined as

$$\delta S = \frac{\frac{dA_{meas}}{dC} - \frac{dA_{sol}}{dC}}{\frac{dA_{sol}}{dC}} \qquad (10\text{-}25)$$

where C is the concentration of the absorbing species (the analyte) in solution and the differentials are the slopes of the analytical curve of A_{meas} or A_{sol} versus C, respectively, and A_{meas} and A_{sol} were previously defined. An expression for the relative increase of sensitivity of absorbance is derived as

$$\delta S = \frac{2r^2t_s^2}{1 - r^2t_s^2} \qquad (10\text{-}26)$$

The calculation of the relative increase of sensitivity of absorbance at 25°C were carried out and are tabulated in Table 10-4 for aqueous and air solutions for fused silica windows.[188,189]

Minimum Concentration Error

The concentration error caused by the transmittance error in the instrumental system due to multiple reflections is defined as

$$E = \frac{1}{dt_{meas}} \left(\frac{dC}{C}\right) \qquad (10\text{-}27)$$

The concentration error caused by the transmittance error is derived as

Table 10-4

Relative Increase of Sensitivity of Absorbance (Parts per Thousand)

	Wavelength (nm)					
	275		468		656	
Measured Transmittance	Aqueous	Air	Aqueous	Air	Aqueous	Air
0.1	0.03	0.17	0.03	0.10	0.03	0.09
0.2	0.14	0.47	0.11	0.38	0.11	0.36
0.3	0.31	1.05	0.25	0.85	0.24	0.81
0.4	0.55	1.87	0.45	1.52	0.43	1.44
0.5	0.86	2.92	0.70	2.37	0.66	2.25
0.6	1.24	4.20	1.01	3.41	0.96	3.23
0.7	1.68	5.71	1.37	4.64	1.30	4.40
0.8	2.20	7.45	1.79	6.06	1.70	5.74
0.9	2.78	9.42	2.27	7.66	2.15	7.26
1.0	3.43	11.62	2.80	9.45	2.66	8.95

$$E = \frac{(1 - r^2 t_s)^2}{(1 - r^2)(1 + r^2 t^2)} \frac{1}{t_s \ln (t_s)} \qquad (10\text{-}28)$$

The minimum values of concentration error (absorber at 25°C) are tabulated in Table 10-5 for aqueous and air solutions for fused silica windows.[188,189]

Relative Increase of Concentration Error at the Same Concentration

The relative increase of concentration error at the same concentration of absorbing species caused by the transmittance error in the instrumental system due to multiple reflections is defined here as

$$\delta E_C = \frac{\frac{1}{dt_{meas}} \left(\frac{dC}{C}\right) - \frac{1}{dt_s} \left(\frac{dC}{C}\right)}{\frac{1}{dt_s} \left(\frac{dC}{C}\right)} \qquad (10\text{-}29)$$

An expression for the relative increase of concentration error at the same concentration is then derived as

$$\delta E_C = \frac{(1 - r^2 t_s^2)^2}{(1 - r)^2 (1 + 4^2 t_s^2)} - 1 \qquad (10\text{-}30)$$

The calculations of the relative increase of concentration error at the same concentration caused by transmittance error in the instrumental system due to multiple reflections (absorber at 25°C) were carried out and are tabulated in Table 10-6 for aqueous and air solutions for fused silica windows.[188,189]

Table 10-5

Minimum Value of Concentration Error

	Wavelength (nm)					
	257		468		656	
	Aqueous	Air	Aqueous	Air	Aqueous	Air
Minimum Concentration Error	2.721	2.728	2.721	2.726	2.720	2.726

Table 10-6

Relative Increase of Concentration Error (Parts per Thousand) at the Same Concentration

Measured Transmittance	Wavelength (nm)					
	275		468		656	
	Aqueous	Air	Aqueous	Air	Aqueous	Air
0.1	1.67	5.63	1.36	4.58	1.29	4.34
0.2	1.51	5.11	1.23	4.15	1.17	3.93
0.3	1.25	4.23	1.02	3.44	0.97	3.26
0.4	0.89	3.00	0.73	2.44	0.69	2.31
0.5	0.43	1.42	0.35	1.16	0.33	1.10
0.6	-0.14	-0.49	-0.11	-0.40	-0.11	-0.38
0.7	-0.81	-2.75	-0.66	-2.23	-0.63	-2.11
0.8	-1.58	-5.34	-1.29	-4.34	-1.22	-4.11
0.9	-2.45	-8.25	-2.00	-6.72	-1.90	-6.37
1.0	-3.42	-11.49	-2.79	-9.36	-2.65	-8.87

Relative Increase of Concentration Error at the Same Transmittance

The relative increase of concentration error at the same transmittance caused by the transmittance error in the instrumental system due to multiple reflections is defined as

$$\delta E_t = \frac{\frac{1}{dt_{meas}}\left(\frac{dC}{C}\right) - \frac{1}{t_{meas}\ln(t_{meas})}}{\frac{1}{t_{meas}\ln(t_{meas})}} \qquad (10\text{-}31)$$

An expression for the relative increase of concentration error at the same transmittance is then derived as

$$\delta E_t = \frac{1 - r^2 t_s^2}{1 + r^2 t_s^2}[1 + A] - 1 \qquad (10\text{-}32)$$

The calculations of the relative increase of concentration error at the same transmittance caused by the transmittance error in the instrumental system due to multiple reflections (absorber at 25°C) were carried out and are tabulated in Table 10-7 for aqueous and air solutions for fused silica windows.[188,189]

Results and Discussion

The results of Table 10-1 are in good agreement with those of Burnett.[176] Our approach is easier to program and has fewer simplifying approximations. The results in Table 10-2 and Table 10-3 are in direct conflict with the results obtained by Hund and Hill, Calvert and Pitts, and Jones and Salisbury.[172,174,175] Their results, which we feel are in error,

Table 10-7

Relative Increase of Concentration Error (Parts per Thousand) at the Same Transmittance

Measured Transmittance	Wavelength (nm)					
	275		468		656	
	Aqueous	Air	Aqueous	Air	Aqueous	Air
0.1	0.70	2.38	0.57	1.94	0.54	1.83
0.2	0.87	3.00	0.72	2.44	0.69	2.31
0.3	0.99	3.34	0.81	2.72	0.76	2.57
0.4	1.02	3.46	0.84	2.81	0.79	2.66
0.5	1.00	3.37	0.81	2.74	0.77	2.60
0.6	0.91	3.08	0.75	2.51	0.71	2.37
0.7	0.77	2.59	0.63	2.11	0.60	2.00
0.8	0.57	1.92	0.47	1.56	0.44	1.48
0.9	0.31	1.05	0.26	0.86	0.24	0.81
1.0	0.00	0.00	0.00	0.00	0.00	0.00

have resulted from their rather gross approximations. When windows of higher indices of refraction were in use, lower limits of detection (see Table 10-1), higher sensitivities of absorbance (see Table 10-4), and less concentration errors (see Table 10-6) could be achieved due to the multiple reflections in absorption spectrophotometry for trace analysis. However, at higher concentrations of absorbind species in solution, concentration errors are increased (see Table 10-6), and the minimum values of concentration error, when multiple reflections within the cell are present, are higher than the conventional minimum value of concentration error, 2.718, when multiple reflections are absent (see Table 10-5). We feel the approach we used can be applied to the study of the distortion of a molecular absorption band due to the frequency-dependent indices of water and of the cell windows.[184]

REFERENCES

1. J. Aitchison and J. A. C. Brown, The Lognormal Distribution, Cambridge University Press, London, 1973.
2. F. Galton, Proc. Roy. Soc., 29, 365 (1879).
3. D. McAlister, Proc. Roy. Soc., 29, 367 (1879).
4. J. C. Kateyn, Skew Frequency Curves in Biology and Statistics, P. Noordhoff Publisher, Groningen, 1903.
5. P. T. Yuan, Ann. Math. Statist., 6, 30 (1933).
6. M. S. Bartlett, J. R. Statist. Soc. Suppl., 4, 137 (1937).
7. P. Allen, Nature, 156, 746 (1945).
8. J. H. Gaddum, Nature, 156, 747 (1945).
9. S. C. Pearce, Nature, 156, 747 (1945).
10. N. L. Johnson, Biometrika, 36, 148 (1949).
11. C. C. Heyde, J. R. Statist. Soc., B, 25, 392 (1963).
12. A. L. Koch, J. Theoret. Biol., 12, 276 (1966).
13. B. W. Lindgren, Statistical Theory, MacMillan, New York, 1968.
14. P. A. P. Moran, Introduction to Probability Theory, Clarendon Press, Oxford, 1968.
15. A. L. Koch, J. Theoret. Biol., 23, 251 (1969).
16. D. B. Siano, J. Chem. Educ., 49, 775 (1972).
17. M. Csorgo, V. Seshadri and M. Yalovsky, J. R. Statist. Soc., B, 35, 507 (1973).
18. K. V. Bury, Statistical Methods in Applied Science, John Wiley and Sons, New York, 1975.
19. P. E. Hart, J. R. Statist. Soc., A, 138, 423 (1975).

20. A. S. Monin and A. M. Yaglom, Statistical Fluid Mechanics, (Ed. J. L. Lumbed), Vol. 1, MIT Press, Cambridge, Mass., 1975.

21. E. P. Weightman, A. P. Trivelli and S. E. Sheppard, J. Phys. Chem., 28, 529 (1924).

22. W. C. Krumbein and E. J. Pettijohn, Manual of Sedimentary Petrography, Appleton-Century, New York, 1938.

23. T. Hatch and S. P. Choate, J. Franklin Inst., 207, 369 (1929).

24. T. Hatch, J. Franklin Inst., 215, 27 (1933).

25. W. C. Krumbein, J. Sediment. Petrol., 6, 35 (1936).

26. A. N. Kolmogoroff, C. R. Acad. Sci. U. R. S. S., 31, 99 (1941).

27. B. Epstein, J. Franklin Inst., 224, 471 (1947).

28. R. P. Loveland and A. P. H. Trivelli, J. Phys. Chem., 51, 1004 (1947).

29. F. Kottler, J. Franklin Inst., 250, 339 (1950).

30. D. G. Krige, J. Chem. Soc. S. Afr., 52, 119 (1951).

31. R. A. Mugele and H. D. Evans, Ind. Eng. Chem., 43, 1317 (1951).

32. F. Kottler, J. Phys. Chem., 56, 442 (1952).

33. G. Herdan, Small-Particle Statistics, Elsevier, Amsterdam, 1953.

34. W. C. Krumbein, J. Amer. Statist. Asso., 49, 51 (1954).

35. W. C. Krumbein and F. A. Graybill, An Introduction to Statistical Models in Geology, McGraw-Hill, New York, 1965.

36. S. Matsumoto and Y. Takashima, Kagaku Kogaku, 33, 357 (1969).

37. S. Matsumoto, Y. Takashima, N. Sakai and Y. Tago, Kagaku Kogaku, 34, 204 (1970).

38. I. Chen, J. Appl. Phys., 45, 4852 (1974).

39. J. C. Kapteyn and M. J. V. Uven, Skew Frequency Curves in Biology and Statistics, Hoitsema Bros., Groningen, 1916.

40. R. Vining, Econometrika, 13, 183 (1945).

41. R. Vining, Econometrika, 14, 37 (1946).

42. G. R. Davies, Econometrika, 14, 219 (1946).

43. J. E. G. Utting and D. E. Cole, Bull. Oxf. Univ. Inst. Statist., 15, 1 (1953).

44. S. J. Prais and J. Aitchison, Rev. Inst. Int. Statist., 22, I/3, 1 (1955).

45. M. F. M. Osborne, Operations Research, 7, 145 (1959).

46. P. J. Dhrymes, Econometrika, 30, 297 (1962).

47. J. S. Cramer, Empirical Economics, North-Holland, Amsterdam, 1971.

48. P. Koller, Marketing Decision Making, Holt, Reinhart and Winston, Englewoods, N.J., 1971.

49. C. R. Nelson, Applied Time Series Analysis, Holden-Day, San Francisco, 1973.

50. S. D. Wicksell, Ark. Mat. Astr. Fys., 12, 20 (1917).

51. A. M. Hemmingsen, Vidensk. Medd. dank. Naturh. Foren Kbh., 98, 125 (1933).

52. C. I. Bliss, Science, 79, 38 (1934).

53. C. I. Bliss, Science, 79, 409 (1934).

54. F. Yates, J. Amer. Statist. Asso., 20, 51 (1934).

55. C. B. Williams, Ann. Appl. Biol., 24, 404 (1937).

56. C. B. Williams, Trans. R. Ent. Soc. Lond., 90, 227 (1940).

57. J. H. Gaddum, Nature, 156, 463 (1945).

58. H. Cramer, Mathematical Methods of Statistics, Princeton University Press, 1946.

59. M. J. V. Uven, Mathematical Treatment of the Results of Agricultural and Other Experiments, P. Noordhoff, Groningen, 1946.

60. J. B. S. Haldane and K. A. Kermack, Biometrika, 37, 30 (1950).

61. P. E. Sartwell, Am. J. Hyg., 51, 310 (1950).

62. L. Bernstein and M. Weatherall, Statistics for Medical and Biological Students, Livingstone, Edinburgh, 1952.

63. M. Feinlieb, J. Am. Statist. Asso., 55, 534 (1960).

64. E. L. Spitznagel, Bioscience, 21, 981 (1971).

65. W. F. F. Kemsley, Ann. Eugen. Lond., 15, 161 (1950).

66. W. F. F. Kemsley, Ann. Eugen. Lond., 16, 316 (1952).

67. W. F. F. Kemsley, Ann. Eugen. Lond., 18, 22 (1953).

68. F. W. Preston, Ecology, 29, 254 (1948).

69. A. Kleczokowski, Ann. Appl. Biol., 36, 139 (1949).

70. H. R. Thompson, Biometrika, 38, 414 (1951).

71. P. M. Grundy, Biometrika, 38, 427 (1951).

72. P. M. Grundy, Biometrika, 39, 252 (1952).

73. L. H. Ahrens, Geochim. Cosmochim. Acta, 5, 49 (1954).

74. F. Chayes, Geochim. Cosmochim. Acta, 6, 119 (1954).

75. L. H. Ahrens, Geochim. Cosmochim. Acta, 6, 121 (1954).

76. L. H. Ahrens, Geochim. Cosmochim. Acta, 11, 205 (1957).

77. L. H. Ahrens, Distribution of the Elements in Our Planet, McGraw-Hill, New York, 1965.

78. L. H. C. Tippett, Shirley Inst. Mem., 13, 35 (1934).

79. B. Epstein, J. Appl. Phys., 19, 140 (1948).

80. K. A. Brownlee, Industrial Experimentation, H. M. S. O., London, 1949.

81. B. B. Day, Rev. Inst. Int. Statist., 17, 129 (1949).

82. P. Delaporte, Rev. Inst. Int. Statist., 18, 161 (1950).

83. M. J. Moreney, Facts from Figures, Penguin, London, 1951.

84. J. Moshman, J. Amer. Statist. Asso., 48, 600 (1953).

85. J. D. Adams, Semiconductor Reliability, 2, 41 (1962).

86. G. J. Hahn and S. S. Shapiro, Statistical Models in Engineering, John Wiley and Sons, New York, 1967.

87. E. Parzen, Time Series Analysis Papers, Holden-Day, San Francisco, 1967.

88. I. B. Gertsbakh and K. B. Kordonski, Models of Failure, Springer Verlag, Berlin, 1967.

89. G. S. Koch and R. F. Link, Statistical Analysis of Geological Data, John Wiley and Sons, New York, 1970.

90. C. I. Bliss, Ann. Appl. Biol., 24, 815 (1937).

91. C. B. Williams, Biometrika, 31, 356 (1940).

92. E. R. Withell, J. Hyg., 42, 124 (1942).

93. W. C. Wake, J. R. Statist. Soc., B, 12, 19 (1950).

94. G. Herdan, Biometrika, 45, 222 (1958).

95. E. U. Condon and G. Breit, Phys. Rev., 49, 229 (1936).

96. H. A. Bethe, Rev. Mod. Phys., 9, 69 (1937).

97. P. Beckmann, J. Res. Natl. Bur. Std. (U. S.) D68, 723 (1964).

98. D. L. Fried, J. Opt. Soc. Am., 57, 169 (1967).

99. D. L. Fried, J. Opt. Soc. Am., 57, 175 (1967).

100. D. L. Fried and J. B. Seidman, J. Opt. Soc. Am., 57, 181 (1967).

101. D. L. Fried, J. Opt. Soc. Am., 57, 268 (1967).

102. D. L. Fried, G. E. Mevers and M. P. Keister, J. Opt. Soc. Am., 57, 787 (1967).

103. D. L. Fried, J. Opt. Soc. Am., 57, 980 (1967).

104 D. A. de Wolf, J. Opt. Soc. Am., 58, 461 (1968).

105. A. Peskoff, J. Opt. Soc. Am., 58, 1032 (1968).

106. Y. Kinoshita, T. Asakura and M. Suzaki, J. Opt. Soc. Am., 58, 1040 (1968).

107. R. L. Mitchell, J. Opt. Soc. Am., 58, 1267 (1968).

108. G. R. Ochs and R. S. Laurence, J. Opt. Soc. Am., 59, 226 (1969).

109. G. R. Ochs, R. R. Bergman and J. R. Snyder, J. Opt. Soc. Am., 59, 231 (1969).

110. P. H. Deitz and N. J. Wright, J. Opt. Soc. Am., 59, 527 (1969).

111. D. A. de Wolf, J. Opt. Soc. Am., 59, 1455 (1969).

112. P. Diament and M. C. Teich, J. Opt. Soc. Am., 60, 1489 (1970).

113. J. R. Kerr, J. Opt. Soc. Am., 62, 1040 (1972).

114. J. W. Strohbehn and T. I. Wang, J. Opt. Soc. Am., 62, 1061 (1972).

115. J. R. Kerr and J. R. Dunphy, J. Opt. Soc. Am., 63, 1 (1973).

116. D. A. de Wolf, J. Opt. Soc. Am., 63, 171 (1973).

117. J. R. Dunphy and J. R. Kerr, J. Opt. Soc. Am., 63, 981 (1973).

118. D. A. de Wolf, J. Opt. Soc. Am., 63, 1249 (1973).

119. D. A. de Wolf, J. Opt. Soc. Am., 64, 360 (1974).

120. T. I. Wang and J. W. Strohbehn, J. Opt. Soc. Am., 64, 583 (1974).

121. T. I. Wang and J. W. Strohbehn, J. Opt. Soc. Am., 64, 994 (1974).

122. F. Davidson and A. Gonzalez-del-Valk, J. Opt. Soc. Am., 65, 655 (1975).

123. V. Blumel, L. M. Narducci and R. A. Tuft, J. Opt. Soc. Am., 62, 1309 (1972).

124. D. B. Siano and D. E. Metzler, J. Chem. Phys., 51, 1856 (1969).

125. D. E. Metzler, C. Harris, I. Y. Yang, D. Siano and J. A. Thomson, Biochem. Biophys. Res. Commun., 46, 1588 (1972).

126. D. B. Siano and D. E. Metzler, J. Chem. Soc., Faraday Trans. II, 268, 2042 (1972).

127. D. E. Metzler, C. M. Harris, R. J. Johnson, D. B. Siano and J. A. Thomson, Biochem., 12, 5377 (1973).

128. I. Y. Yang, R. M. Khomutov and D. E. Metzler, Biochem., 13, 3877 (1974).

129. I. Y. Yang, C. M. Harris, D. E. Metzler, W. Korytnyk, B. Lackmann and P. P. G. Potti, J. Biol. Chem., 250, 2957 (1975).

130 H. A. Laitinen, Chemical Analysis, McGraw-Hill, New York, 1960.

131. R. V. Mises, Mathematical Theory of Probability and Statistics, Academic Press, New York, 1964.

132. S. Chandrasekhar, Rev. Mod. Phys., 15, 1 (1943).

133. S. Goldman, Information Theory, Dover, New York, 1953.

134. J. B. Thomas, An Introduction to Applied Probability and Random Processes, John Wiley and Sons, New York, 1971.

135. E. Kreyszig, Introductory Mathematical Statistics, John Wiley and Sons, New York, 1970.

136. G. U. Yule and M. G. Kendall, An Introduction to the Theory of Statistics, Charles Griffin, London, 1947.

137. W. Feller, An Introduction to Probability Theory and Its Applications, Vol. 1, John Wiley and Sons, New York, 1957.

138. L. J. Curtis, Am. J. Phys., 43, 1101 (1975).

139. R. A. Kahn, Am. Math. Monthly, 81, 366 (1974).

140. A. Sommerfeld, Optics (Transl. O. Laport and P. A. Moldauer), Academic Press, New York, 1954.

141. A. Sommerfeld, Thermodynamics and Statistics (Transl. J. K. Kestin), Academic Press, New York, 1956.

142. A. Yariv, Quantum Electronics, John Wiley and Sons, New York, 1975.

143. L. S. Ornstein and W. R. V. Wyk, Zs. f. Phys., 78, 734 (1932).

144. T. P. Sheahen and T. O. McCanney, J. Opt. Soc. Am., 65, 825 (1975).

145. A. P. Thorne, Spectrophysics, John Wiley and Sons, New York, 1974.

146. J. Shuster, Am. Statistics, 27, 29 (1973).

147. B. A. Lengyel, Lasers, Wiley Interscience, New York, 1971.

148. C. Kittel, Elementary Statistical Physics, John Wiley and Sons, New York, 1958.

149. F. P. Chen, Electric Probes in Plasma Diagnostic Techniques (Ed. R. H. Huddlestone and S. L. Leonard), Academic Press, New York, 1965.

150. J. D. Swift and M. J. R. Schwar, Electric Probes for Plasma Diagnostic, Elsevier, New York, 1969.

151. R. Avni and J. D. Winefordner, Spectrochim. Acta, 30 B, 281 (1975).

152. E. Parzen, Modern Probability and Its Applications, John Wiley and Sons, New York, 1960.

153. S. J. Strickler and R. A. Berg, J. Chem. Phys., 37, 814 (1962).

154. M. W. Hanna, Quantum Mechanics in Chemistry, W. A. Benjamin, New York, 1966.

155. M. Okazaki, I. Hara and T. Fujiyama, J. Phys. Chem., 80, 64 (1976).

156. V. P. Klochkov and V. L. Bogdanov, Opt. Spectrosc., 29, 458 (1970).

157. J. D. Winefordner, S. G. Schulman and T. C. O'Haver, Luminescence Spectrometry in Analytical Chemistry, Wiley Interscience, New York, 1972.

158. H. H. Jaffe and J. T. D'Agostino, J. Chem. Educ., 47, 14 (1970).

159. W. H. Fink, J. Chem. Educ., 48, 544 (1971).

160. S. L. Ross, Differential Equations, p. 384, Xerox College, Lexington, Mass., 1974.

161. H. C. Ramsperger, Proc. Natl. Acad. Sci., 13, 849 (1927).

162. J. A. Rubin and S. V. Filseth, J. Chem. Educ., 46, 57 (1969).

163. J. V. Venerus and T. E. Bullock, Nucl. Sci. Eng., 40, 199 (1970).

164. S. Glasstone, Thermodynamics for Chemists, Van Nostrand, New York, 1947.

165. J. W. Strutt, Scientific Papers by Lord Rayleigh (John William Strutt), Vol. II, p. 199, Dover, New York, 1964.

166. R. E. Langer, Phys. Rev., 51, 669 (1937).

167. R. A. Day and A. L. Underwood, Quantitative Analysis, p. 64, Prentice-Hall, Englewood Cliffs, New Jersey, 1967.

168. K. P. Li, D. L. Duewer and R. S. Juvet, Anal. Chem., 46, 1209 (1974).

169. S. D. Nogare and R. S. Juvet, Gas-Liquid Chromatography, Interscience, New York, 1962.

170. P. Rosin and E. Rammler, J. Inst. Fuel, 7, 29 (1933).

171. S. Nukiyama and Y. Tanasawa, Trans. Soc. Mech. Engrs., 4, No. 14, 86 (1938).

172. G. M. Hieftje and H. V. Malmstadt, Anal. Chem., 40, 1860 (1968).

173. B. J. Mason, The Physics of Clouds, p. 25, Oxford University Press, London, 1971.

174. N. A. Fuchs and A. G. Sutigen, Highly Dispersed Aerosols, p. 86, Ann Arbor Science Publishers, Ann Arbor, 1970.

175. N. K. Adam, The Physics and Chemistry of Surfaces, p. 14, Dover, New York, 1968.

176. A. C. Manzies, Anal. Chem., 32, 898 (1960).

177. C. E. Lapple, Advances in Chemical Engineering (Ed. T. B. Drew, G. R. Cokelet, J. W. Hoopes and T. Vermulen), Vol. VIII, p. 1, Academic Press, New York, 1970.

178. R. E. Hund and T. L. Hill, J. Chem. Phys., 15, 111 (1947).

179. L. S. Goldring, R. C. Hawes, G. H. Hare, A. O. Beckman and M. E. Strickney, Anal. Chem., 25, 869 (1953).

180. J. G. Calvert and J. N. Pitts, Photochemistry, p. 793, John Wiley and Sons, New York, 1960.

181. S. H. Jones and K. Salisbury, Photochem. Photobiol., 16, 435 (1972).

182. R. W. Burnett, Anal. Chem., 45, 383 (1973).

183. J. D. Winefordner and R. C. Elser, Anal. Chem., 43, No. 5, 24A (1971).

184. N. Omenetti, L. P. Hart and J. D. Winefordner, Appl. Spectrosc., 26, 612 (1972).

185. N. Omenetti, L. P. Hart, P. Benetti and J. D. Winefordner, Spectrochim. Acta, 28B, 301 (1973).

186. Optical Fused Quartz and Fused Silica, Amersil, Hillside, New Jersey.

187. P. Kaiser, A. R. Tynes, H. W. Astle, A. D. Pearson, W. G. French, R. E. Jaeger and A. H. Cherin, J. Opt. Soc. Am., 63, 1149 (1973).

188. E. W. Washburn, International Critical Tables, Vol. VII, p. 13, McGraw-Hill, New York, 1930.

189. I. H. Malitson, J. Opt. Soc. Am., 55, 1205 (1965).

190. B. V. Lopatin and T. E. Kuznetsova, Zavodskaya Laboratoriya, 37, 1455 (1971).

BIOGRAPHICAL SKETCH

Che Ted Chen was born on January 6, 1943. He attended public schools and high school in Taiwan. After he graduated with the Bachelor of Science degree from the National Taiwan University in June 1966, he worked in quality control for one year and pharmaceutical analysis for another year. In June 1970, he received the Master of Science degree from the same university. He began to work for the Ph. D. degree at the University of Florida in September 1970.

He married the former Margaret K. Y. Wong and is the father of twins, Liza and Timothy.

I certify that I have read this study and that in my opinion it conforms to acceptable standards of scholarly presentation and is fully adequate, in scope and quality, as a dissertation for the degree of Doctor of Philosophy.

James D. Winefordner, Chairman
Professor of Chemistry

I certify that I have read this study and that in my opinion it conforms to acceptable standards of scholarly presentation and is fully adequate, in scope and quality, as a dissertation for the degree of Doctor of Philosophy.

Roger G. Bates
Professor of Chemistry

I certify that I have read this study and that in my opinion it conforms to acceptable standards of scholarly presentation and is fully adequate, in scope and quality, as a dissertation for the degree of Doctor of Philosophy.

Kuang-Pang Li
Assistant Professor of Chemistry

I certify that I have read this study and that in my opinion it conforms to acceptable standards of scholarly presentation and is fully adequate, in scope and quality, as a dissertation for the degree of Doctor of Philosophy.

Dinesh O. Shah

Dinesh O. Shah
Professor of Chemical Engineering

I certify that I have read this study and that in my opinion it conforms to acceptable standards of scholarly presentation and is fully adequate, in scope and quality, as a dissertation for the degree of Doctor of Philosophy.

R. Carl Stoufer

R. Carl Stoufer
Associate Professor of Chemistry

This dissertation was submitted to the Graduate Faculty of the Department of Chemistry in the College of Arts and Sciences and to the Graduate Council, and was accepted as partial fulfillment of the requirements for the degree of Doctor of Philosophy

December 1976

Dean, Graduate School